Original Research

GDF15 and LCN2 for early detection and prognosis of pancreatic cancer

Xinxia Zhu [a,b], Brennan Olson [a,c,d], Dove Keith [b], Mason A Norgard [a], Peter R Levasseur [a,b], Parham Diba [a,b,c], Sara Protzek [b], Ju Li [a], Xiaolin Li [a,e], Tetiana Korzun [a,c], Ariana L Sattler [a,b,f], Abigail C Buenafe [a], Aaron J Grossberg [b,g,h], Daniel L Marks [a,b,f,*]

[a] *Papé Family Pediatric Research Institute, Oregon Health & Science University, Portland, Oregon, USA*
[b] *Brenden-Colson Center for Pancreatic Care, Oregon Health & Science University, Portland, Oregon, USA*
[c] *Medical Scientist Training program, Oregon Health & Science University, Portland, Oregon, USA*
[d] *Department of Otolaryngology-Head and Neck Surgery, Mayo Clinic, Rochester, Minnesota, USA*
[e] *Nutritional Biology, Division of Human Nutrition, Wageningen University, Wageningen, Netherlands*
[f] *Knight Cancer Institute, Oregon Health & Science University, Portland, Oregon, USA*
[g] *Department of Radiation Medicine, Oregon Health & Science University, Portland, Oregon, USA*
[h] *Cancer Early Detection Advanced Research Center, Oregon Health & Science University, Portland, Oregon, USA*

ARTICLE INFO

ABSTRACT

Background: The prognosis of pancreatic ductal adenocarcinomas (PDAC) remains very poor, emphasizing the critical importance of early detection, where biomarkers offer unique potential. Although growth differentiation factor 15 (GDF15) and Lipocalin 2 (LCN2) have been linked to PDAC, their precise roles as biomarkers are uncertain.
Methods: Circulating levels of GDF15 and LCN2 were examined in human PDAC patients, heathy controls, and individuals with benign pancreatic diseases. Circulating levels of IL-6, CA19-9, and neutrophil-to-lymphocyte ratio (NLR) were measured for comparisons. Correlations between PDAC progression and overall survival were assessed. A mouse PDAC model was employed for comprehensive analyses, complementing the human studies by exploring associations with various metabolic and inflammatory parameters. Sensitivity and specificity of the biomarkers were evaluated.
Findings: Our results demonstrated elevated levels of circulating GDF15 and LCN2 in PDAC patients compared to both healthy controls and individuals with benign pancreatic diseases, with higher GDF15 levels associated with disease progression and increased mortality. In PDAC mice, circulating GDF15 and LCN2 progressively increased, correlating with tumor growth, behavioral manifestations, tissue and molecular pathology, and cachexia development. GDF15 exhibited highly sensitive and specific for PDAC patients compared to CA19-9, IL-6, or NLR, while LCN2 showed even greater sensitivity and specificity in PDAC mice. Combining GDF15 and LCN2, or GDF15 and CA19-9, enhanced sensitivity and specificity.
Interpretation: Our findings indicate that GDF15 holds promise as a biomarker for early detection and prognosis of PDAC, while LCN2 could strengthen diagnostic panels.

Introduction

The prognosis for patients with pancreatic ductal adenocarcinomas (PDAC), the most common type of pancreatic cancer, remains very poor. The 5-year survival rate is only 12.5 %, with minimal improvement since the 1960s and the poorest prognosis among common solid malignancies [1–3]. Currently, it is the third leading cause of cancer-related deaths, but recent statistics on incidence and survival indicate that by 2030,

PDAC will likely become the second leading cause of cancer-related mortality in the United States [4,5]. Several critical factors contribute to these unfavorable outcomes, including diagnosis at a late-stage, limited surgical candidacy, aggressive metastatic behavior, drug resistance, and a high incidence of cachexia [6,7]. Strategies aimed at improving early detection hold great promise for enhancing survival rates by increasing the number of patients eligible for surgical resection, the only potentially curative treatment [2,5]. However, despite

---

* Corresponding author.
E-mail address: dan@endevicabio.com (D.L. Marks).

extensive worldwide research on over 1000 potential cancer biomarkers, none are established as the definitive gold-standard diagnostic biomarker for PDAC. [8,9]

There has been significant focus on identifying circulating biomarkers that could provide a minimally invasive approach for PDAC surveillance [10,11]. Currently used circulating biomarkers, such as CA19-9, CEA, and CA125, have limitations in sensitivity and specificity for detecting PDAC [2,12]. For example, CA19-9, a tetrasaccharide expressed on the surface of cancer cells, is the most recognized serological biomarker for pancreatic cancer diagnosis. However, it lacks the necessary sensitivity and specificity, especially in healthy individuals and those with benign conditions [13]. Consequently, CA19-9 is of limited value for early detection of PDAC, as elevated levels typically indicate advanced disease rather than early-stage cancer, particularly when the tumor is less than 3 cm in diameter [12]. Furthermore, CA19-9 elevation is observed in only 80 % of pancreatic cancer patients, and 10 % of those with a Le (α-β-) phenotype do not produce CA19-9 protein [8, 9].

GDF15, a divergent member of the transforming growth factor (TGF)-ß superfamily, was initially identified in activated macrophages [14]. It is broadly expressed in various tissues under normal conditions and is significantly upregulated in response to oxidative stress, inflammation, tissue damage, and cancer. As a member of the TGF-ß super family and a stress-associated cytokine, GDF15 influences tumorigenesis and cancer development through multiple pathways, including Smad and non-Samd pathways as well as other receptors [15,16]. In the early stages of cancer, GDF15 can induce tumor cell apoptosis and inhibit cancer progression, while in the later stages, it may promote tumor cell proliferation and metastasis [15,17]. Research has demonstrated a strong link between GDF15 and pancreatic cancer. [18–20]. Furthermore, during cancer progression, GDF15 triggers metabolic activities that suppress appetite and promote fat loss and muscle atrophy via activating the glial cell-derived neurotrophic factor receptor alpha-like (GFRAL) in the brainstem and other GDF15 receptors or pathways [15,21–23]. Both human and animal studies have revealed that elevated levels of circulating GDF15 are correlated with anorexia, wight loss, cachexia, and decreased survival rates [24–29]. Given the higher incidence of cachexia associated with PDAC, [7,30] GDF15 plays a crucial role in influencing PDAC progression and outcomes. Therefore, it is rational to further investigate whether GDF15 could serve as a biomarker throughout the course of the disease.

LCN2, also known as neutrophil gelatinase-associated lipocalin or oncogene 24p3, is primarily expressed in neutrophils and plays a role in innate immunity by sequestering iron and preventing its use by bacteria to limit their growth [31]. Elevated circulating LCN2 is associated with anorexia in response to inflammatory and metabolic processes during various diseases, including cancer, chronic kidney disease and heart failure [32–37]. Our previous work demonstrated that in PDAC, circulating and cerebrospinal fluid LCN2 levels are elevated and correlated with anorexia, tissue wasting, low survival, and hippocampal neuronal dysfunction-associated cognitive impairment [38–40]. Another study suggested that LCN2 modulates the secretion of pro-inflammatory cytokines in pancreatic cancer stellate cells, key mediators of the abundant PDAC stroma [33]. Furthermore, a recent study demonstrated high LCN2 levels in patient blood and brain metastases in multiple cancer types, associated with disease progression and poor survival [41]. Based on these observations and considering the context where LCN2 predominantly originates from neutrophils, including those within the tumor microenvironment (tumor-associated neutrophils), we hypothesize that LCN2 plays an active role in pancreatic tumor growth and metastasis during the early stages. Consequently, LCN2 holds promise as a remarkably sensitive biomarker for PDAC.

Although GDF15 and LCN2 were discovered many years ago and have been associated with cancer, reports from translational studies remain limited despite the increasing number of review articles in the literature. In the present work, we reasoned that both circulating GDF15 and LCN2 could serve as biomarkers for early detection and prognosis of PDAC, due to their strong associations with cancer-related immunity and metabolism. We sought to determine the role of GDF15 and LCN2 as biomarkers for PDAC early detection, disease progression monitoring, and prognostication. We first examined the circulating levels of GDF15 and LCN2 in healthy subjects and individuals with PDAC or benign pancreatic diseases, and explored the relationship between GDF15 and LCN2 levels and disease progression, cachexia development, and overall survival (OS). In addition, we compared GDF15 and LCN2 with the commonly employed biomarkers including CA19-9, IL-6, and neutrophil-to-lymphocyte ratio (NLR). To further test our hypothesis in complementing the human studies, we then utilized a well-documented mouse model of PDAC, and comprehensively examined correlations between the GDF15 and LCN2 levels and pancreatic tumor growth, behavioral manifestations, tissue and molecular pathological characteristics, and cancer cachexia phenotypes. Finally, we conducted an evaluation of sensitivity and specificity to ascertain whether GDF15 and LCN2 exhibit higher sensitivity and specificity for PDAC in comparison to other commonly employed biomarkers.

Materials and methods

Acquisition of human samples and clinical data

Serum samples were obtained from individuals aged 22–89 years, diagnosed with pancreatic ductal adenocarcinoma (PDAC) or various benign pancreatic diseases in the Brenden-Colson Center for Pancreatic Care in Portland, Oregon, USA, through the Oregon Pancreatic Tumor Registry (OPTR, IRB3609). These samples were collected at the time of diagnosis and, in some cases, during follow-up visits. Healthy control samples from age- and sex-matched individuals without clinical evidence of PDAC were procured from the Oregon Clinical and Translational Research Institute Research Volunteer Registry (IRB 10709). These control patients underwent a similar clinical evaluation as the pancreatic cancer group at Oregon Health & Science University (OHSU) but were found to have no evidence of pancreatic disease. Blood was drawn through venipuncture and serum was isolated and stored at −80 °C until analysis. Samples were collected with participant informed consent to the above studies. The use of these retrospective and anonymized human samples and data in this project did not require Institutional Review Board (IRB) approval as they were considered non-human subject research.

Computed-tomography-based body composition analysis

Access to CT scans was approved by the OHSU IRB, and all patients had provided consent for the OPTR protocol. For each patient, a single contrast-enhanced axial image at the third lumbar vertebra (L3) was selected, anonymized, and saved in DICOM format using Osirix v11.0 (Pixmeo). An automated algorithm in MATLAB R2016a (MathWorks) was used for first-pass segmentation [42], identifying and labeling skeletal muscle and visceral fat based on their established radiodensity ranges (−29 to +150 and −190 to −30 Hounsfield Units, respectively) [43,44]. The images underwent manual corrections using Sliceomatic 5.0 (Tomovision). Skeletal muscle index (SMI) and normalized visceral fat measures for each patient were calculated by dividing the total cross-sectional area of skeletal muscle and fat at L3 (in cm^2) by the square of the patient's height (in m^2).

Mice

Male C57BL/6J (Stock# 000,664) mice were obtained from The Jackson Laboratory (Bar Harbor, ME, USA). They were housed in our animal facility with controlled conditions, including a temperature of 25 °C and a 12-h light-dark cycle. The mice had ad libitum access to water and food (Purina rodent diet 5001; Purina Mills, St. Louis, MO, USA).

After being individually housed for at least 7 days for acclimation, mice aged of 9–10 weeks were used in all experiments. Prior to the procedures, mice were randomly grouped but balanced based on their initial body weights. Tumor-bearing mice were euthanized according to the endpoints set by the tumor study policy. All experiments were conducted following the guidelines of the National Institutes of Health Guide for the Care and Use of Laboratory Animals and were approved by the Institutional Animals Care and Use Committee of OHSU.

Tumor cell culture and implantation

The PDAC mouse model was generated using a KPC cell line (generously provided by Dr. Elizabeth Jaffee) derived from C57BL/6J mice, in which the pancreas-specific conditional alleles KRAS^{G12D} and TP53R^{172H} were expressed under the Pdx-1-Cre promoter. Since the KPC model is well-characterized and extensively published for its ability to replicate key features of the PDAC disease process [45], we utilized this model in all mouse studies. The KPC cells were cultured in RPMI 1640 medium supplemented with 10 % fetal bovine serum, 1 % minimum essential medium non-essential amino acids, 1 mM sodium pyruvate, and 1 % penicillin/streptomycin (Gibco, Gaithersburg, MD, USA) at 37 °C in a cell incubator with 5 % CO_2. The KPC cell line was regularly tested and confirmed to be free of mycoplasma contamination. Before implantation, the cells were harvested, counted, and aliquoted to ensure a consistent number of cells to be implanted in each animal. Under isoflurane anesthesia, a small longitudinal incision was made in the upper-left quadrant of the abdomen to expose the pancreas. 0.7 million KPC cells suspended in 30 μL of PBS were injected into the tail of the pancreas without leakage using a Hamilton syringe. Mice in the sham groups were injected with an equal volume of PBS. Following the implantation, the abdominal wall muscle layer was sutured, and the skin incision was securely closed with two surgical staples.

Food intake and body weight measurement

In the mouse studies, we measured food intake and body weight manually daily at a similar time point (3 h after lights on) from the day of implantation (day 0) until the day of euthanasia. To ensure accurate measurement of food intake, we accounted for the loss of uningested food caused by sick mice, which produced considerable food spillage (orts or crumbs) as the experiments progressed. Daily food orts were screened from the cage bedding and quantified throughout the study. We also monitored the animals' overall health condition daily.

Locomotor activity measurement

To assess voluntary home cage locomotor activity (LMA), we utilized a MiniMitter system (MiniMitter, Bend, OR, USA), as previously described [30]. Briefly, under isoflurane anesthesia, MiniMitter transponders for sensing LMA were implanted subcutaneously, and the animals were then returned to their home cages. We recorded LMA in the *x*-axis, *y*-axis and *z*-axis in 5-minute intervals throughout the entire experimental period.

Body composition analysis

Body composition (fat mass and lean mass) was analyzed twice on the day of implantation and the end of study prior to tissue collection via EchoMRI (4-in-1, Live Animal Composition Analyzer; Echo Medical System, Houston, TX, USA).

Blood glucose test and tissue collection

When the tumor-bearing animals reached the predetermined criteria for euthanasia or specific terminal time points, we conducted blood glucose testing using a OneTouch meter and strips (LifeScan Europe,

Zug, Sweetland), immediately before the terminal MRI scan. The animals were then deeply anesthetized with a ketamine-xylazine-acepromazine cocktail, and blood was collected via cardiac puncture into an EDTA blood collection tube for hematology assay. After the hematology assay, plasma was isolated, aliquoted, and stored at −80 °C until analysis. Brain tissue was extracted and the hypothalamus was dissected. Additionally, we dissected and weighed the heart, spleen, pancreas, brown adipose tissue (BAT), inguinal white adipose tissue (iWAT), gonanal white adipose tissue (gWAT), and tumor. Furthermore, we dissected and weighed the quadriceps, gastrocnemii, tibialis anterior and solei of both left and right hindlimbs. For molecular analysis, all tissues were snap-frozen immediately after dissection with liquid nitrogen and stored at −80 °C until further analysis. Tissues intended for histopathology analysis were fixed with 4 % paraformaldehyde.

Hematology assay

Whole blood was subjected to analysis using a veterinary hematology analyzer (HemaVet, 950FS, Drew Scientific, Oxford CT, USA) to measure various hematological parameters, including total leucocyte counts, leucocyte differential (neutrophils, lymphocytes, monocytes, eosinophils, and basophils), erythrocytes, hemoglobin concentration, hematocrit, mean corpuscular volume, mean corpuscular hemoglobin, mean corpuscular hemoglobin concentration, and thrombocytes.

Enzyme-linked immunosorbent assay (ELISA)

Concentrations of GDF15, LCN2, and IL-6 in patient serum and mouse plasma were determined using enzyme-linked immunosorbent assay (ELISA) kits following the manufacturers' instructions (R&D Systems, catalog # DY957, DY1757-05, DY206-05, DY6385-05, DY1857-05, DY406-05). Human CA19-9 in patient serum was also measured using ELISA kits as per the manufacturers' instructions (RayBiotech, ELH-CA19-9-2).

Histopathology

Paraformaldehyde fixed tumor tissues were submitted to the OHSU Histopathology Core for preparation of paraffin-embedded and hematoxylin & eosin (H&E) stained histological sections. The stained representative tumor sections (three sections with higher neutrophil counts per animal, three animals per group) were evaluated by a specialist who was blinded to the experimental groups. Neutrophil counts of three tumor tissue sections in each animal were quantified and averaged, and total 3 animals of each group (each time point) were evaluated. Representative fields were photographed.

Real-time quantitative PCR

Frozen tissues were rapidly homogenized, and RNA was extracted using the RNeasy Mini Kit (Qiagen). Subsequently, the RNA samples were reverse-transcribed using the High-Capacity cDNA Reverse Transcription Kit (Life Technologies). Real-time quantitative PCR (qRT-PCR) was conducted using reagents (Life Technologies) and an ABI 7300 (Applied Biosystems). TaqMan primer probes listed in Supplemental Table 2 were utilized for the qRT-PCR. The expression levels of the target genes in the tissues were normalized to either *18 s* or *Actb* using the ddCt method.

Ethics

The use of the retrospective and anonymized human samples and data did not require Institutional Review Board (IRB) approval, as they were considered non-human subject research. Mouse studies were approved by the IACUC of the Oregon Health & Science University and conducted according to the NIH Guide for the Care and Use of

Laboratory Animals (National Academies Press, 2011).

Statistical analysis

Statistical analyses for the data from mouse studies were conducted using GraphPadPrism 10.0 software. Quantitative data are reported as mean ± standard error (mean ± SEM). To compare two groups with normally distributed data, a two-tailed unpaired Student *t*-test was used, whereas for non-normally distributed data, a nonparametric test (Mann-Whitney test) was employed. When comparing more than two groups, one-way analysis of variance (ANOVA) was utilized. For comparing multiple time points and treatment groups (sham vs. tumor), unless otherwise specified in the figure legends, two-way ANOVA with Tukey's multiple comparisons test was used. Before performing correlation analysis, normality was confirmed using Shapiro-Wilk tests, and for data following a Gaussian distribution, Pearson correlation was applied for parametric data. Data from the human studies, obtained from exported Excel files, were analyzed using GraphPad Prism 10.0 and IBM SPSS Statistics Suite (version 25). Kaplan-Meier survival curve comparisons were conducted using the Log-rank Mantel-Cox test. To determine the optimal cutpoints for dichotomizing patient serum levels of GDF15, LCN2, IL-6, CA19-9, or NLR and their association with survival outcomes, we used the Evaluate Cutpoints adaptive algorithm software in RStudio. This approach follows the previously published application and guidelines established by Ogłuszka, M., and collegues, as detailed in the publication [46]. The application utilizes R language, incorporating algorithms from packages such as survival and optimal cutpoints, and provides Kaplan-Meier plots and receiver operating characteristic (ROC) curves for cutoff point determination. ROC curves were constructed to assess sensitivity, specificity, and the corresponding areas under the curves (AUCs) with 95 % confidence intervals. Single and integrated biomarker ROC curve analyses were conducted using logistic regression. To assess the sensitivity and specificity of the combined biomarkers through integrated ROC analysis, R version 4.2.1 (R Core Team, 2022) was used to calculate "LR yhat" values for the dual-marker ROC curves. Each LR yhat value was based on a pair of matched test results (GDF15-CA19-9 and GDF15-LCN2) from each individual or mouse. This analysis was conducted by a statistical specialist from Biostatistics Shared Resource Core at the Knight Cancer Institute, OHSU (see Acknowledgements section). All ROC curves, including integrated ones, were graphed using GraphPad Prism 10.0. Statistical significance was considered at a p-value of < 0.05 for all data analyses. Histochemistry analyses were based on images representing at least three separate stainings, with all measurements taken from distinct samples to ensure no duplication from the same samples.

Results I: human studies

Circulating GDF15 and LCN2 are elevated and associated in patients with PDAC

In the human studies, we examined the levels of circulating GDF15 and LCN2 in patients with PDAC and compared them with that in healthy subjects (healthy control) and individuals with benign pancreatic diseases (benign PD). We analyzed 249 serum samples from PDAC patients, 42 from healthy subjects, and 138 from benign PD patients (Supplemental Table 1). Both GDF15 and LCN2 levels in PDAC patients were significantly increased compared to healthy and benign PD subjects (Fig. 1, a and b). In addition, because IL-6 has been extensively investigated as a potential diagnostic biomarker of PDAC [47–49], we measured IL-6 levels in the same serum samples. The levels of circulating IL-6 were found to be predominantly variable or undetectable in PDAC, healthy, and benign PD groups, although a significant difference between PDAC and benign PD groups was detected (Fig. 1c). The correlation analysis demonstrated a strong association between circulating levels of GDF15 and LCN2 in PDAC patients, whereas there was no correlation between healthy and benign PD subjects (Supplemental Fig. 1a). Furthermore, the GDF15 levels were correlated with IL-6 levels within all three groups (Supplemental Fig. 1b), while there was no correlation between the LCN2 and IL-6 levels among the three groups (Supplemental Fig. 1c). To further assess the diagnostic potential of GDF15 and LCN2, we compared serum levels with CA19-9, a commonly
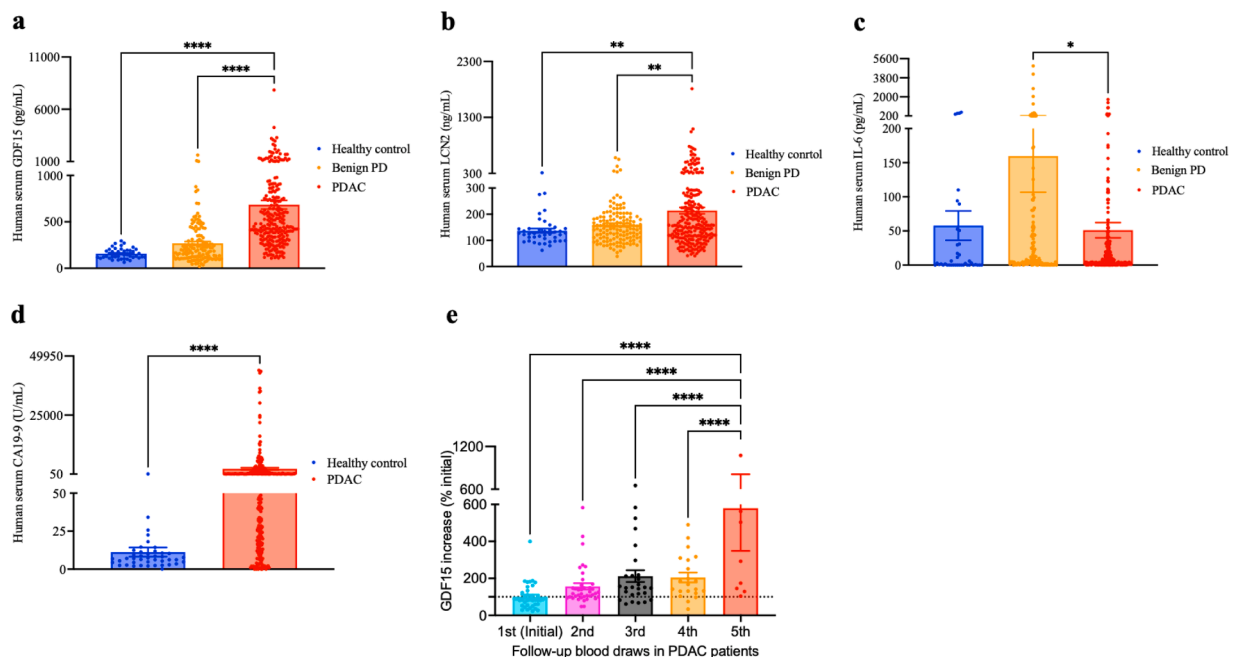

Fig. 1. Circulating GDF15 and LCN2 are elevated and associated in patients with PDAC. Serum concentrations of GDF15 (a), LCN2 (b), and IL-6 (c) in patients with PDAC or benign pancreatic diseases (PD), and healthy controls. (d) Serum CA19-9 concentrations in PDAC patients and healthy controls. (e) Serum GDF15 level changes in PDAC patients with multiple follow-up blood draws. Data in (a-e) are expressed with each dot representing one sample. (a-d) Healthy control group, *n* = 42, benign PD group, *n* = 138, PDAC groups, *n* = 249. (e) PDAC group, *n* = 9–39. *$P < 0.05$; **$P < 0.01$; ****$P < 0.0001$. One-way ANOVA (a-c) and (e). Mann-Whitney test (d).

used serological biomarker for PDAC [9,50,51]. While serum CA19-9 levels were significantly higher in PDAC patients compared to healthy controls (Fig. 1d), there was no significant correlation between the levels of GDF15, LCN2, IL-6, and CA19-9 (Supplemental Fig. 1, d-f). Additionally, we explored the blood NLR, which has been considered for early cancer detection and prognosis assessment [52–54]. We observed an increased NLR (average > 3) in PDAC patients (Supplemental Fig. 1g), which was positively correlated with circulating LCN2 levels but not significantly associated with GDF15, IL-6 or CA19-9 levels (Supplemental Fig. 1, h-k). In patients with PDAC who underwent multiple consecutive blood tests, we observed a progressive rise in serum GDF15 levels (Fig. 1e, Supplemental Fig. 1l). Collectively, these results indicate that circulating GDF15 and LCN2 hold unique diagnostic and prognostic value for PDAC, independent of other commonly employed biomarkers such as CA19-9, IL-6, and NLR.

Circulating GDF15 levels are correlated to poor survival in patients with PDAC

To elucidate the connection between circulating GDF15 and LCN2 levels and the prognosis of PDAC, we explored their relationship with survival rates in PDAC patients. Following the approach detailed by Ogłuszka, M. et al. [46], we set cutoff values for different biomarkers and identified the associated thresholds: 535.9 pg/mL for GDF15, 112.3 ng/mL for LCN2, 25.73 pg/mL for IL-6, 56.9 U/mL for CA19-9, and 5.25 for NLR. These values enabled the categorization of patients according to their survival outcomes in univariate analysis. Within our patient cohort, PDAC patients with serum GDF15 levels at or above 535.9 pg/mL at the time of blood collection exhibited significantly reduced overall survival (OS) probability compared to those with GDF15 levels below this threshold (Fig. 2a). However, we did not observe a significant difference in the OS probability between patients with serum LCN2 levels at or above 112.3 ng/mL or IL-6 levels at or above 25.73 pg/mL, compared to those with levels below these thresholds (Fig. 2, b and c), respectively. Furthermore, the probability of OS showed no variance among patients with serum CA19-9 levels equal to, exceeding, or falling

below 56.9 U/mL (Fig. 2d). In addition, when analyzing the association between the OS probability and blood NLR at various cutoff values (3.1, 3.5, 4.0 and 5.25) based on previous reports [52,55,56], we found no significant correlation between reduced OS and increased NLR (Fig. 2e, specifically comparing NLR < 5.25 vs NLR ≥ 5.25). As cachexia is a critical driver for mortality, we evaluated muscle and fat depletion in PDAC patients. Based on previous reports suggesting that local CT scan-derived muscle measurements can predict outcomes in advanced cancer patients [43,44], we quantified skeletal muscle and visceral adipose tissue using axial images at the third lumbar vertebrae upon PDAC diagnosis. Surprisingly, we found no notable association between serum levels of GDF15 or LCN2 and skeletal muscle index (SMI) or visceral fat in PDAC patients (Supplemental Fig. 2, a-d).

Results II: mouse studies

Association of circulating GDF15 and LCN2 with pancreatic tumor growth in mice

To examine the association of circulating GDF15 and LCN2 levels with pancreatic tumor growth, we conducted a time-course study using a mouse model of pancreatic KPC tumor, involving four specific end time points (Fig. 3a). Mice were euthanized on day 4, 7, 10 and 14 after orthotopic implantation of KPC pancreatic tumor cells or PBS (sham control). Tumors were meticulously dissected and weighed at the respective time points. Representative tumors from each time point were also imaged (Fig. 3b). The tumor mass exhibited logarithmic growth over the course of the study (Fig. 3c, Supplemental Fig. 3a). We assayed plasma samples for GDF15, LCN2, and IL-6 concentrations. Notably, the circulating levels of GDF15, LCN2 and IL-6 showed progressive increases following KPC tumor growth throughout the disease course. Specifically, the GDF15 levels were markedly elevated in the tumor mice at day 10 and 14 compared to the sham-control mice (Fig. 3d), while the LCN2 levels displayed a significant increase starting from day 4 after KPC tumor implantation (Fig. 3e). The circulating IL-6 was detectable in most of KPC tumor-bearing mice but not in the sham-control mice. The IL-6
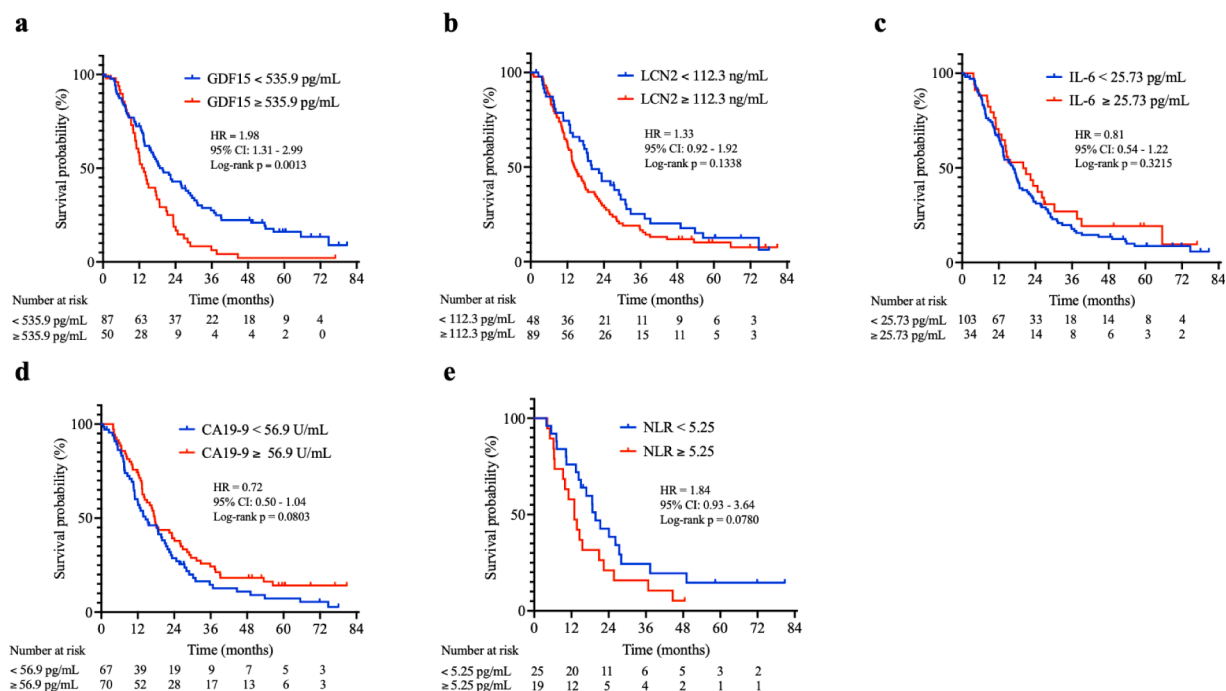

Fig. 2. Circulating GDF15 levels are correlated to poor survival in patients with PDAC. Overall survival probability in patients with pancreatic cancer dichotomized by levels of 535.9 pg/mL GDF15 (a), 112.3 ng/mL LCN2 (b), 25.73 pg/mL IL-6 (c), 56.9 U/mL CA19-9 (d), and 5.25 NLR (e) at diagnosis. $n = 137$ (a-d), $n = 44$ (e). All data in (a-e) are analyzed by the Log-rank Mantel-Cox test (two sided).
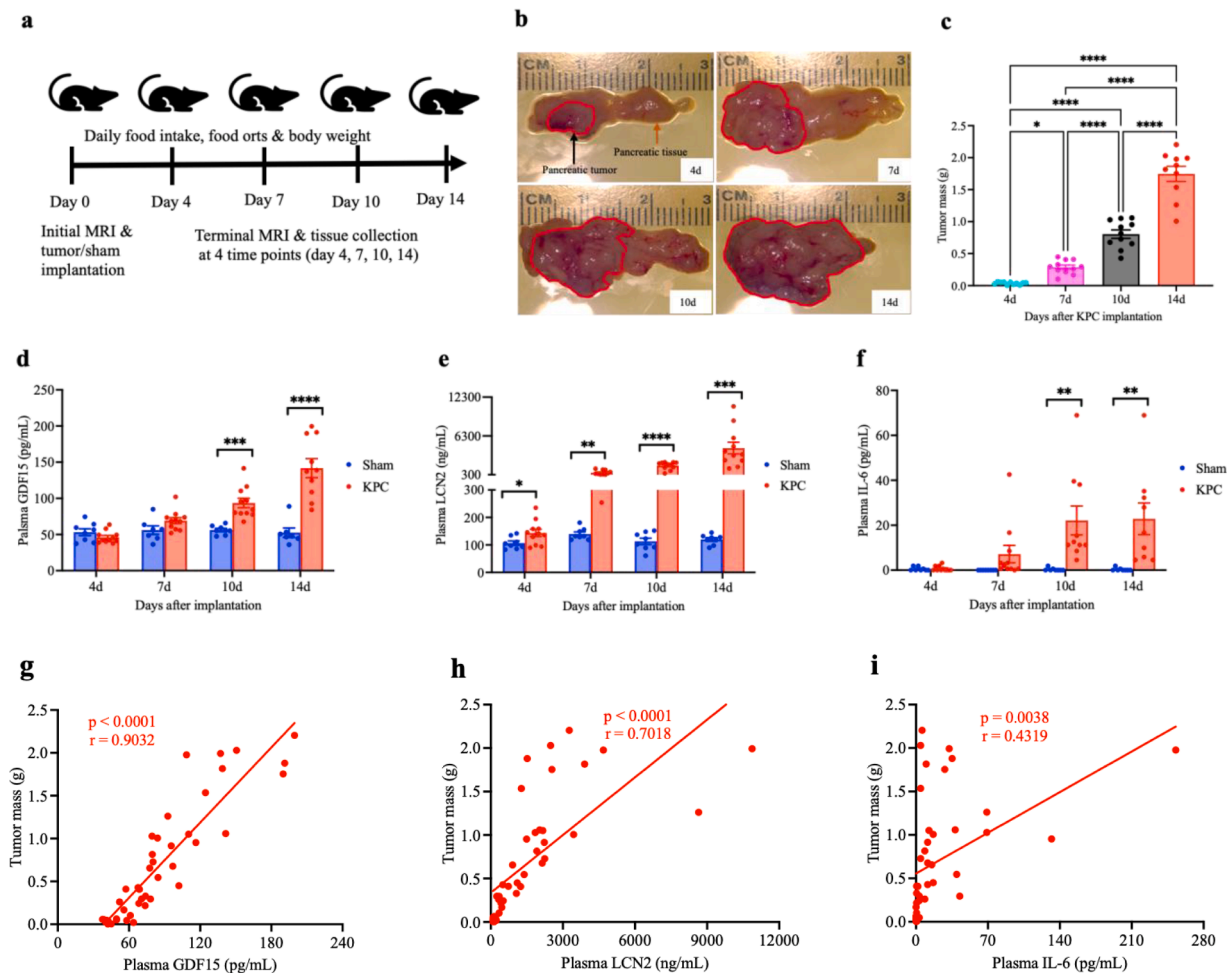
Fig. 3. Association of circulating GDF15 and LCN2 with pancreatic tumor growth in mice. (a) Schematic of experimental procedures: orthotopic implantation of KPC tumor cells or sham-operation, time points for measurement of food intake, orts (food spillage), body weight, and body composition by MRI, and for euthanasia and tissue collection. (b) Tumor size, and (c) Tumor mass at 4 time points (day 4, 7, 10, and 14) after implantation of KPC cells. Plasma levels of GDF15 (d), LCN2 (e), and IL-6 (f). (g-i) Correlations between plasma GDF15, LCN2, IL-6 levels and tumor mass. All data in (c-i) are expressed with each dot representing one sample. (c-f) Sham group, $n = 7-8$, KPC tumor group, $n = 10-11$. (g-i) Sham group, $n = 30$, KPC tumor group, $n = 43$. $*P < 0.05$; $**P < 0.01$; $***P < 0.001$; $****P < 0.0001$. One-way ANOVA (c). Unpaired Student's t-test for each pair (KPC vs sham) at each time point (d-f). Pearson correlation coefficient and linear regression-fitting curves (g-i).

levels were increased in the tumor mice at day 10 and 14, although the degree of increase varied (Fig. 3f). Furthermore, the circulating levels of GDF15, LCN2 and IL-6 were found to be positively correlated with tumor mass (Fig. 3, g-i). Moreover, in the tumor mice, a strong association was observed between GDF15 and LCN2 levels, while no significant correlation was found with IL-6 levels (Supplemental Fig. 3, b and c). Additionally, a correlation was observed between circulating LCN2 and IL-6 levels (Supplemental Fig. 3d).

Elevation of circulating GDF15 and LCN2 is linked to the severity of anorexia, body mass loss, and fatigue in PDAC mice

To determine how increased circulating GDF15 and LCN2 correspond to anorexia, body weight loss, and reduced physical activity during pancreatic cancer progression, we closely monitored daily food intake, body weight change, and movement pattern throughout the disease course. During the mid-stage of the disease, we observed sickness behaviors in KPC tumor-bearing mice, including anorexia, weight loss, and decreased physical activity (fatigue), which accurately reproduced the common clinical manifestations of PDAC. Furthermore, the tumor mice exhibited a distinct behavior wherein they crunched more food pellets, resulting in a considerable amount of food orts (crumbs or food spillage that the animals did not ingest), likely due to discomfort

and stress following cancer progression. To precisely measure food intake, we daily screened the cage bedding for food orts. Notably, the tumor mice produced substantially and progressively more food orts than the sham control mice (Supplemental Fig. 4a). After accounting for food orts, there was no significant change in daily food intake between the tumor and sham mice until day 9 post-implantation. All eight sham and KPC groups had similar daily food intake during the first 8 days of the disease course (Fig. 4a). Nevertheless, cumulative food intake in the tumor mice started to decline on day 10 and remained consistently lower compared to the sham mice (Supplemental Fig. 4b). By day 10 and 14, total food intake was significantly reduced in the tumor mice compared to the sham mice (Fig. 4b). The correlation analysis revealed a noteworthy connection in the tumor mice between decreased food intake and elevated levels of GDF15 starting from day 10 and LCN2 on day 14, while no such connection was found with IL-6 (Fig. 4c). We also monitored the body weights throughout the entire time course. Due to variations in tumor mass and ascites during the cancer progression, gross body weights in living KPC tumor mice showed fluctuations (Supplemental Fig. 4c) that precluded meaningful interpretation. Instead, using an EchoMRI body composition analyzer, we measured whole body composition in living mice for fat mass and lean mass prior to tumor or sham implantation (initial MRI) and just before euthanasia and tissue collection (terminal MRI). The final net change of each type of tissue was
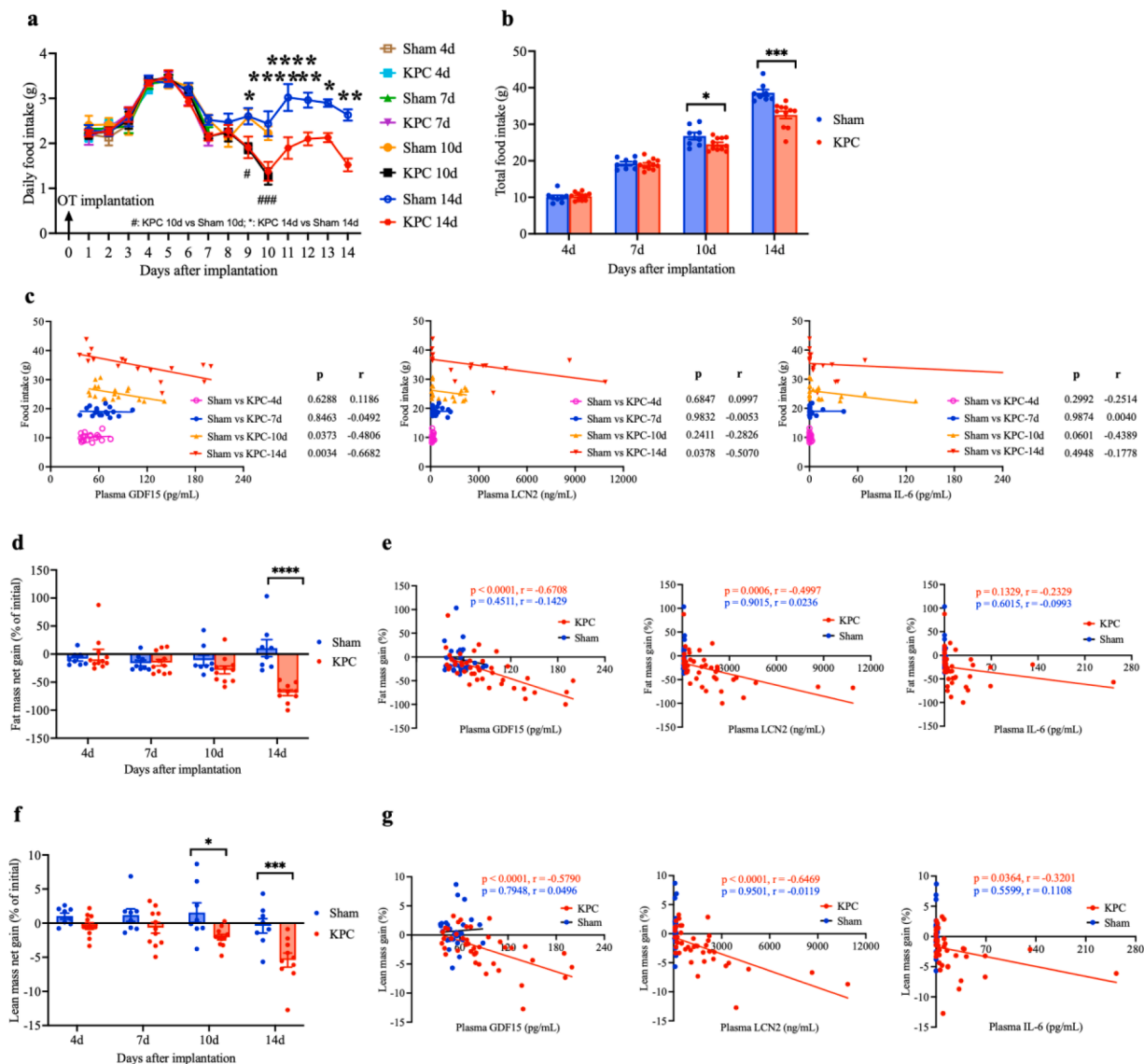
Fig. 4. Elevation of circulating GDF15 and LCN2 is linked to the severity of anorexia, body mass loss, and fatigue in PDAC mice. (a) Daily food intake after orthotopic implantation of KPC tumor cells or sham-operation. (b) Total food intake in sham and KPC tumor mice. (c) Correlations between plasma GDF15, LCN2, IL-6 levels and total food intake at each time point. (d) Fat mass net gain. (e) Correlations between plasma GDF15, LCN2, IL-6 levels and fat mass net gain. (f) Lean mass net gain. (g) Correlations between plasma GDF15, LCN2, IL-6 levels and lean mass net gain. (h) In a separate experiment for locomotor activity measurement, locomotor activity in dark (active) phase and light (inactive) phase before and after KPC tumor implantation or sham-operation. 12-hour movement counts were summed for dark phase and light phase of each day. (i) Locomotor activity changes in dark and light phase. (j) Correlations between plasma GDF15, LCN2, IL-6 levels and dark phase movement. All data in (a), (h), and (i) are expressed as mean ± SEM for each group, and all data in (b-g) and (j) are expressed with each dot representing one sample. (a-d) and (f), sham group, $n = 7$–8, KPC group, $n = 10$–11. (e), (g), and (j), sham group, $n = 30$, KPC group, $n = 43$. (h) and (i), sham group, $n = 10$, KPC group, $n = 10$. *$P < 0.05$; **$P < 0.01$; ***$P < 0.001$; ****$P < 0.0001$. Two-way ANOVA (a), (h), and (i). Unpaired Student's t-test for each pair (KPC vs sham) at each time point (b), (d), and (f). Pearson correlation coefficient and linear regression-fitting curves (c), (e), (g), and (j).

normalized to the initial tissue mass. KPC tumor mice showed a slight loss of fat mass on day 10 and a substantial loss on day 14 (Fig. 4d, Supplemental Fig. 4d). The reduction in fat mass showed a significant association with the increased levels of circulating GDF15 and LCN2, while there was no notable correlation with IL-6 (Fig. 4e). The lean mass was significantly reduced in 10d and 14d KPC mice compared to sham mice (Fig. 4f, Supplemental Fig. 4e). Once more, a robust correlation was observed between the decline in lean mass and the rise in circulating GDF15 and LCN2 levels, with no significant association found for IL-6 (Fig. 4g). In a separate mouse study, using a MiniMitter system we continuously monitored the daily activity, recording their movement at 5-minute intervals throughout the disease course. Similar to the time-course study, the key features of PDAC were replicated in this 14-day

MiniMitter study (Supplemental Fig. 4, f-i). The total movement during 12-h dark phase (mouse active phase) showed a gradual decrease in KPC tumor mice as the disease advanced (Fig. 4h), but there was no significant change observed during light phase (mouse sleep phase, Fig. 4h). To account for the variability in daily activity among individual animals, we analyzed the relative change in the movement counts. KPC tumor mice showed decreased activity (relative to baseline) in the dark phase starting from day 6 post-tumor implantation (Fig. 4i), indicating that fatigue is an early detectable symptom during PDAC progression. Moreover, KPC tumor mice exhibited decreased activity relative to baseline during light phase on day 9, 12, and 13 compared to the sham mice (Fig. 4i). A pronounced connection was observed between the fatigue progression and the elevation of circulating levels of GDF15, LCN2,
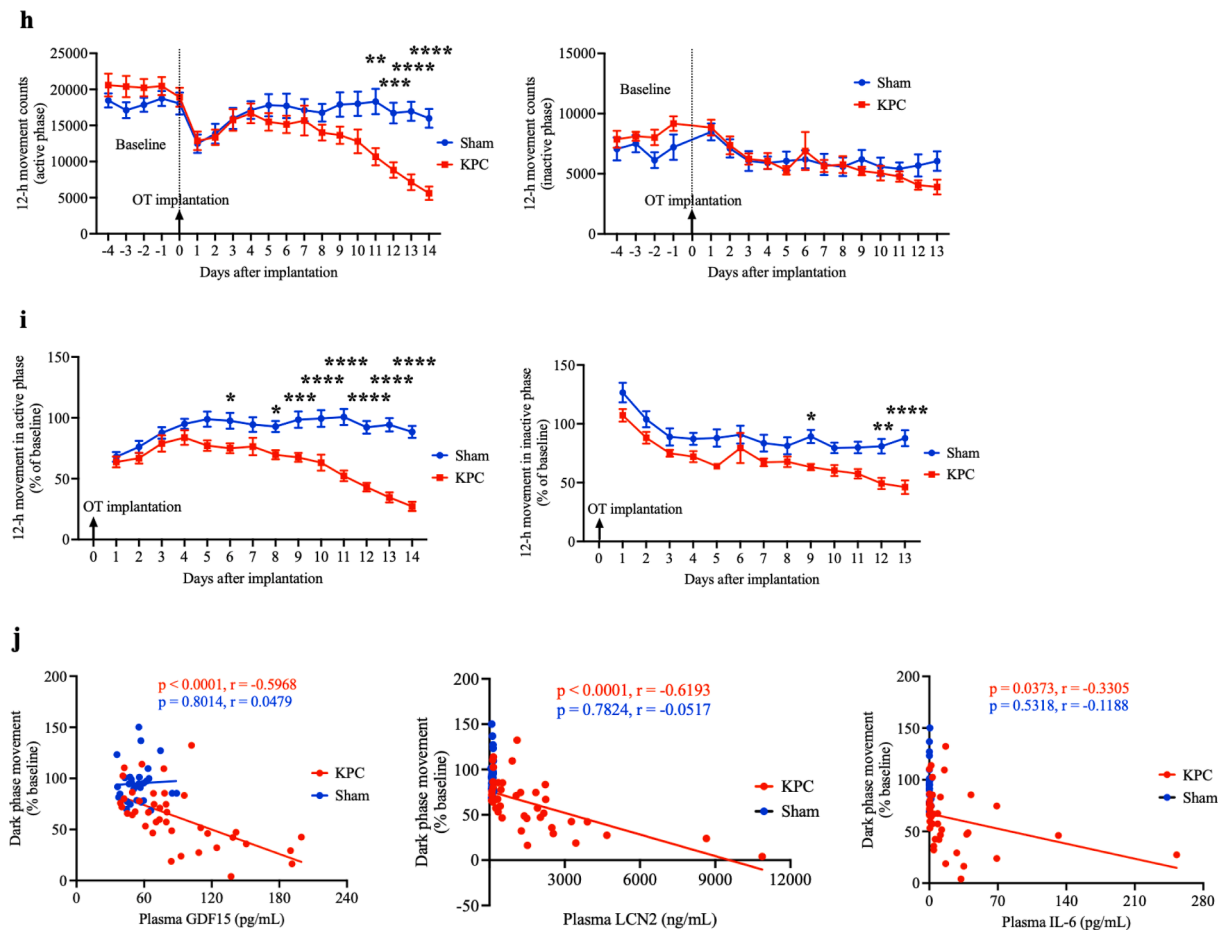
Fig. 4. (*continued*).

and IL-6 (Fig. 4j). Taken together, these results suggest a strong correlation between the occurrence and severity of anorexia, body mass reduction, and fatigue, coupled with the gradual increase in circulating GDF15 and LCN2, dependent on the progression of the disease.

Elevation of circulating GDF15 and LCN2 is associated with fat and muscle wasting in PDAC mice

To explore the wasting of fat and muscle tissues in the PDAC mice during disease progression, we examined two-type fat tissues and two-type muscle tissues. The brown adipose tissue (BAT) showed a progressive decrease in KPC tumor mice compared to the sham mice, starting at day 7 after tumor implantation, and this reduction reached significance on day 14 (Fig. 5a, Supplemental Fig. 5a). Similarly, the white adipose tissues, including inguinal and gonadal adipose tissues (iWAT and gWAT), were reduced on day 14 in KPC mice compared to sham mice, but the change in iWAT did not reach significance due to variability (Fig. 5, b and c, Supplemental Fig. 5, b and c). A notable correlation was detected between the reduction in gWAT and the increase in circulating levels of GDF15 and LCN2, while no significant association was found with IL-6. (Fig. 5d). The cardiac muscle wasting in KPC tumor mice was notably more pronounced than in the sham mice (Fig. 5e, Supplemental Fig. 5d). This wasting process showed a significant connection with the elevation of circulating GDF15 levels, whereas there was no notable correlation with LCN2 or IL-6 (Fig. 5f). Out of the four-type examined skeletal muscle tissues (quadriceps, tibialis anterior, soleus, and gastrocnemius), the quadriceps, tibialis anterior, and gastrocnemius muscles displayed substantial reductions in 10d and 14d KPC tumor mice compared to the sham mice, while the soleus muscle did not exhibit a similar decrease (Fig. 5, g-j, Supplemental Fig. 5, e-h).

Correlation analyses unveiled a robust relationship between the atrophy of the gastrocnemius muscle and the increase in circulating levels of GDF15 and LCN2, with no such corresponding association found for IL-6 (Fig. 5k). Furthermore, in our analysis of the gastrocnemii for muscle catabolic gene transcripts, we observed upregulated mRNA expression levels of *Mafbx, Murf*, and *Foxo1* in 10d and 14d KPC tumor mice relative to the sham mice (Fig. 5l). In addition, KPC tumor mice at 10d and 14d displayed reduced blood glucose levels compared to the sham mice (Fig. 5m), which was linked to the increase in circulating levels of GDF15, LCN2, and IL-6 (Fig. 5n).

Severity of systemic, local, and central inflammation is linked to the elevation of circulating GDF15 and LCN2 in PDAC mice

Given the critical role of GDF15 as a cytokine and LCN2 as a pleiotropic inflammatory mediator, which are both associated with cancer initiation, progression, metastasis, and cachexia development, we examined the relationship between the severity of systemic, local, and central inflammation and the elevated levels of circulating GDF15 and LCN2, and also compared to the circulating IL-6 and NLR levels. In the hematological analysis of blood samples collected from the time-course study, we observed a progressive increase in white blood cells (WBC) and neutrophils during disease progression. Specifically, 10d and 14d KPC tumor mice exhibited remarkably higher WBC and neutrophil counts, with no significant change in lymphocytes, monocytes, eosinophils, and basophils compared to the sham mice (Fig. 6a). Moreover, the neutrophil ratio in KPC tumor mice was robustly increased starting from day 7 after tumor implantation, while the lymphocyte ratio was decreased (Supplemental Fig. 6a). The NLR exhibited a remarkable increase in KPC tumor mice at the 7d, 10d, and 14d when compared to the
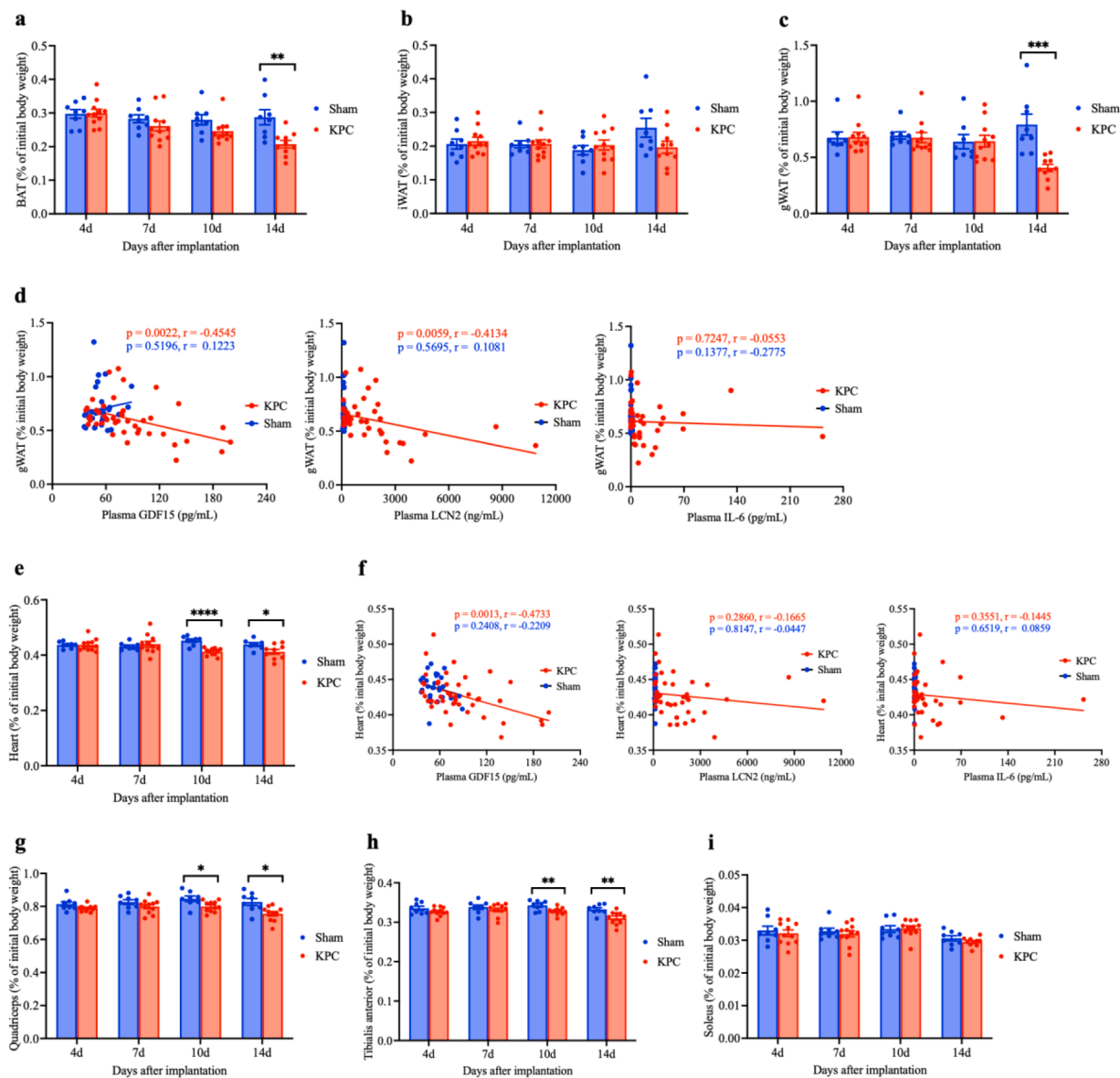
Fig. 5. Elevation of circulating GDF15 and LCN2 is associated with fat and muscle wasting in PDAC mice. (a) Brown adipose tissue (BAT), (b) Inguinal adipose tissue (iWAT), and (c) Gonadal adipose tissue (gWAT) weights. (d) Correlation between plasma GDF15, LCN2, IL-6 levels and gWAT mass. (e) Heart mass. (f) Correlations between plasma GDF15, LCN2, IL-6 levels and heart mass. (g) Quadriceps. (h)Tibialis. (i) Soleus mass. (j) Gastrocnemius mass. (k) Correlations between plasma GDF15, LCN2, IL-6 levels and gastrocnemius mass. (l) Gene expression in gastrocnemii. (m) Terminal blood glucose levels. (n) Correlations between plasma GDF15, LCN2, IL-6 levels and blood glucose levels. All data in (a-n) are expressed with each dot representing one sample. $*P < 0.05$; $**P < 0.01$; $***P < 0.001$; $****P < 0.0001$. Unpaired Student's *t*-test for each pair (KPC vs sham) at each time point in (a-c), (e), (g-j), (l), and (m), sham group, $n = 7$–8, KPC group, $n = 10$–11. Pearson correlation coefficient and linear regression-fitting curves in (d), (f), (k), and (n), sham group, $n = 30$, KPC group, $n = 43$.

sham mice (Fig. 6b), and it displayed a pronounced positive correlation with GDF15 and LCN2 levels, while no such correlation was observed with IL-6 levels (Fig. 6c). Other notable changes in hematology parameters included lower hemoglobin (Hb) concentrations in 14 KPC mice and lower hematocrit (HCT) in 4d, 10d, and 14d KPC tumor mice compared to the sham mice (Supplemental Fig. 6b). Furthermore, thrombocyte counts were significantly decreased in 4d, 7d and 10d KPC mice relative to sham mice (Supplemental Fig. 6c). In addition, the spleen weight progressively increased in KPC mice compared to sham mice during the course of the disease (Fig. 6d, Supplemental Fig. 6d), indicating an increased severity of tumor-induced splenomegaly. To assess the severity of inflammation in the tumor microenvironment, we analyzed tumor tissues collected from 4d, 7d, 10d and 14d KPC mice respectively (Fig. 3, b and c). Histological hematoxylin and eosin (H&E)

staining revealed progressive infiltration of tumor cells into the pancreas, the gradual disappearance of normal pancreatic cells including islets, and escalating neutrophil infiltration surrounding pancreatic tissue and tumor cells as the disease advanced (Fig. 6e). Particularly, 10d and 14d KPC tumors exhibited massive neutrophils (labeled with cyan arrows) and inflamed neutrophils (labeled with red arrows) (Fig. 6e). Infiltrated neutrophils in KPC tumors were significantly increased over the course of the disease (Fig. 6f). To further validate the inflammatory activities within the tumor microenvironment, we analyzed pancreatic and tumor tissues in 14d sham and KPC tumor mice for several inflammatory gene transcripts. *Gdf15, Tgfb1, Lcn2, Ccl2, Tnf, and Il6* mRNA expression levels were upregulated in the KPC pancreas relative to sham pancreas, and the mRNA expression levels of these genes were even higher in the tumor tissue (Fig. 6g),
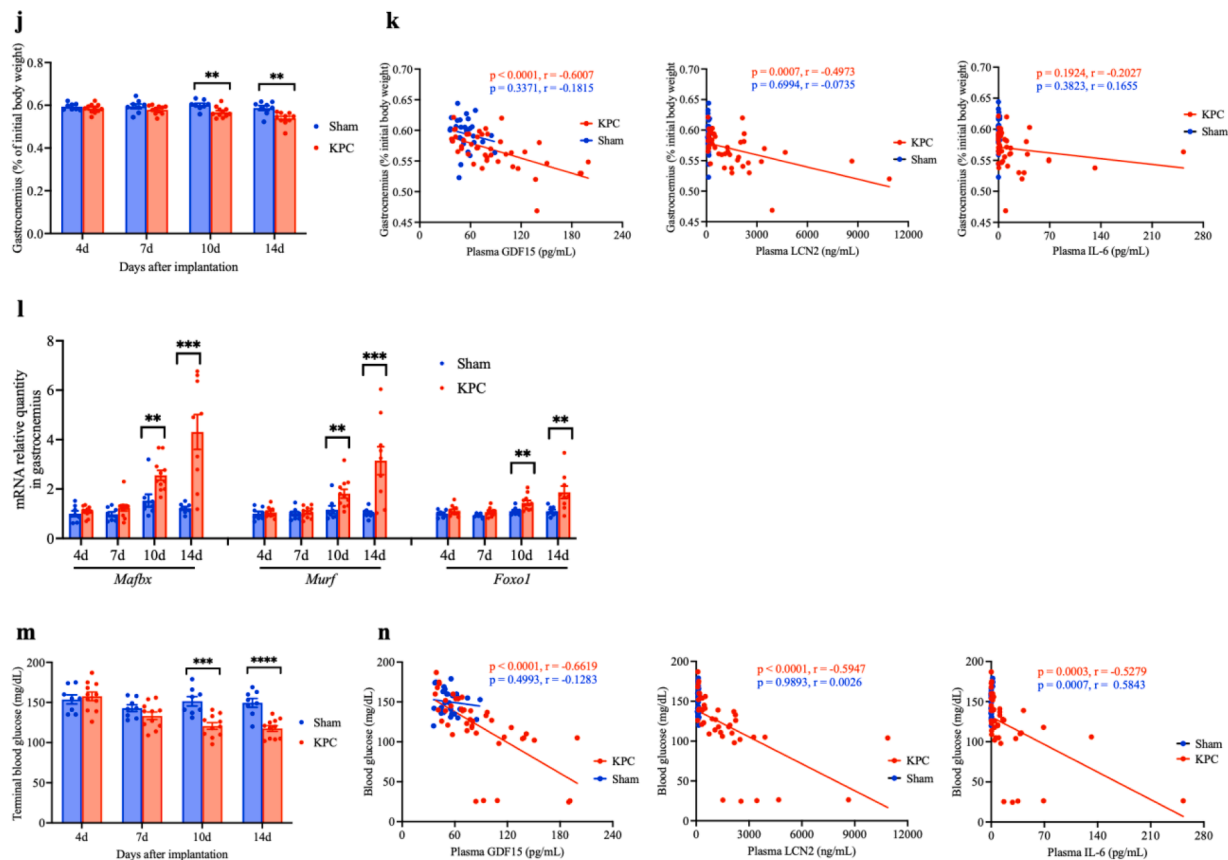
Fig. 5. (*continued*).

indicating inflamed organ and tumor microenvironment. Interestingly, we observed increased *Ifnb1* mRNA expression in KPC mouse pancreas but not tumor tissue, suggesting a role for this molecule in local tumor invasion (Fig. 6g). Finally, we examined the severity of inflammation in the central nervous system (CNS) by analyzing the hypothalamic tissue for several inflammatory gene transcripts. The mRNA expression levels of *IL1b* and *Il1r1* were progressively upregulated in KPC tumor mice relative to sham mice over the course of the disease (Fig. 6h). Interestingly, while *Lcn2* expression in the hypothalamus was remarkably upregulated in mice after bearing KPC tumor for 7 days, the *Gdf15* expression levels did not change in KPC tumor mice compared to sham mice (Fig. 6h).

Assessment of sensitivity and specificity of circulating GDF15 and LCN2 for patients and mice with PDAC

To further elucidate the potential biomarker role of circulating GDF15 and LCN2 in the early detection and prognosis of PDAC, we analyzed their sensitivity and specificity in both patients and mice with PDAC compared to controls. Furthermore, since no gold-standard biomarkers for PDAC have been established, it is essential to compare GDF15 and LCN2 with the most widely used and extensively studied non-gold-standard biomarkers to assess their clinical relevance. These analyses provide meaningful insights and clinical implications [57]. We compared the sensitivity and specificity of GDF15 and LCN2 with the widely used biomarker CA19-9. In the human cohort, the area under the receiver operating characteristic (ROC) curve (AUC) for GDF15 was 0.9458 (95 % CI, 0.9210 to 0.9706, Fig. 7a), for LCN2 it was 0.6352 (95 % CI, 0.5624 to 0.7079, Fig. 7b), and for CA19-9 it was 0.8472 (95 % CI, 0.8007 to 0.8937, Fig. 7c). Moreover, we performed integrated AUC analyses for the three biomarkers (GDF15, LCN2, and CA19-9) measured from the same samples. The integrated AUC for GDF15 and CA19-9 was

0.9664 (95 % CI, 0.9481 to 0.9848), while the integrated AUC for GDF15 and LCN2 was 0.9481 (95 % CI, 0.9238 to 0.9723, Fig. 7d), indicating that combining GDF15 with either CA19-9 or LCN2 increased sensitivity and specificity. In the mouse cohort, the AUC for GDF15 was 0.7620 (95 % CI, 0.6518 to 0.8722) (Fig. 7e), while for LCN2, it was 0.9217 (95 % CI, 0.8564 to 0.9870) (Fig. 7f). The integrated AUC for GDF15 and LCN2 was 0.9527 (95 % CI, 0.9110 to 0.9944, Fig. 7g). Remarkably, the AUC of GDF15 in human PDAC outperformed LCN2, while conversely, the AUC of LCN2 in mouse PDAC was superior to GDF15. These findings collectively suggest that both circulating GDF15 and LCN2 have the potential to distinguish patients with PDAC from healthy subjects, with GDF15 showing greater sensitivity and specificity compared to LCN2 and CA19-9.

Discussion

Mechanistic studies revealed that GDF15 and LCN2 play crucial roles in responding to various physiological and pathophysiological conditions, and directly influence hierarchical regulation systems involved in appetite, energy balance, and metabolism in the central nervous system (CNS) through distinct signaling pathways. GDF15 via GFRAL and LCN2 via the central melanocortin system [17,38]. This suggests that GDF15 and LCN2 hold potential as diagnostic biomarkers and therapeutic targets. Studies in humans and animals show that elevated levels of circulating GDF15 are highly correlated with several types of malignancies [17]. Similarly, several recent studies reported an association between circulating LCN2 and certain types of cancer [33,38,41]. However, the precise relationship between circulating GDF15 and LCN2 and their dynamics during PDAC progression remains unclear. Additionally, it is uncertain whether GDF15 and LCN2 can independently serve as diagnostic and prognostic biomarkers for early detection, progression monitoring, and outcome prediction in PDAC. In this study, we
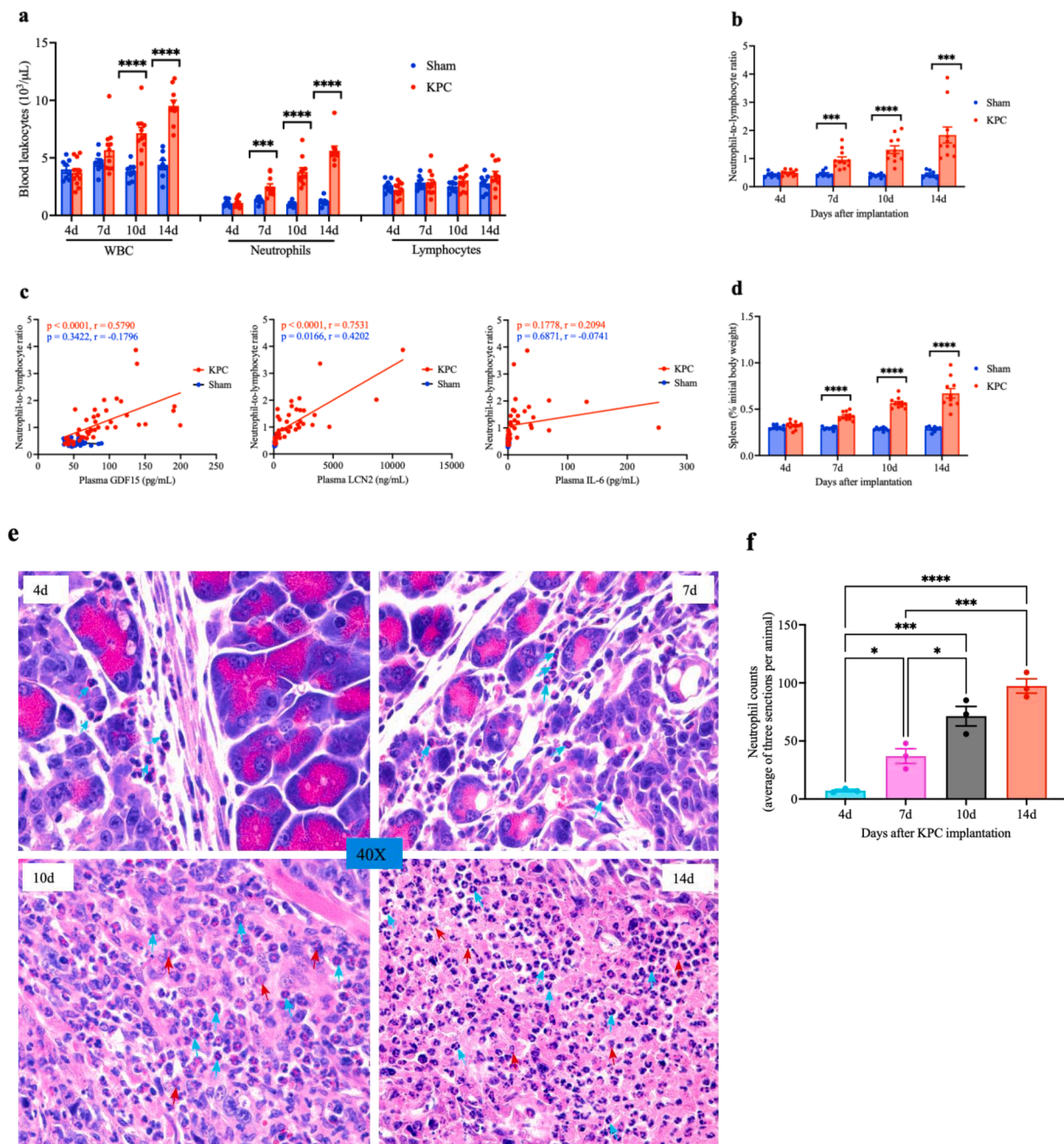
Fig. 6. Severity of systemic, local, and central inflammation is linked to the elevation of circulating GDF15 and LCN2 in PDAC mice. (a) Blood leukocyte counts. (b) Blood neutrophil-to-lymphocyte ratio (NLR). (c) Correlation between plasma GDF15, LCN2, IL-6 levels and blood NLR. (d) Spleen weight. (e) Representative pancreatic tumor sections with H&E staining. 40X magnification with a light microscope, arrows in cyan indicate normal neutrophils and arrows in red indicate inflamed neutrophils. (f) Infiltrated neutrophil counts in tumor site. Summed neutrophil counts of three tumor tissue sections in each animal were quantified and averaged, and 3 animals from each group (each time point) were evaluated. (g) Gene expression in pancreatic tissue and pancreatic tumor at day 14 time point. (h) Gene expression in the hypothalamus. Sham group, $n = 7–8$, KPC group, $n = 10–11$. All data in (a-d) and (f-h) are expressed with each dot representing one sample. (a), (b), (d), and (h), sham group, $n = 7–8$, KPC group, $n = 10–11$. (c) sham group, $n = 30$, KPC group, $n = 43$. (f), KPC group, $n = 3$. (g) Sham-pancreas group, KPC-pancreas group, KPC-tumor group, $n = 7$. *$P < 0.05$; **$P < 0.01$; ***$P < 0.001$; ****$P < 0.0001$. Unpaired Student's *t*-test for each pair (KPC vs sham) at each time point (a), (b), (d), and (h). Pearson correlation coefficient and linear regression-fitting curves (c). One-way ANOVA (f) and (g).

firstly addressed these questions in humans. We observed significant elevations of circulating GDF15 and LCN2 in PDAC cohort compared with the healthy and benign cohorts, and the elevations particularly GDF15 levels were correlated to PDAC progression and OS. We also noted increased CA19-9 levels in the same PDAC cohort and increased IL-6 levels in the benign cohort, consistent with previous reports [50,51, 58–62]. Furthermore, GDF15 levels strongly correlated with LCN2 levels

only within the PDAC cohort, and also correlated with IL-6 levels in all three cohorts. However, neither GDF15 nor LCN2 levels were associated with CA19-9 levels, suggesting independent roles of GDF15 and LCN2 in PDAC.

Regarding limitations and inherent challenges of human studies, such as incomplete information and sub-optimal controlled conditions, animal studies offer unique advantages to overcome these shortcomings.

g Gene expression in pancreatic tissue and pancreatic tumor
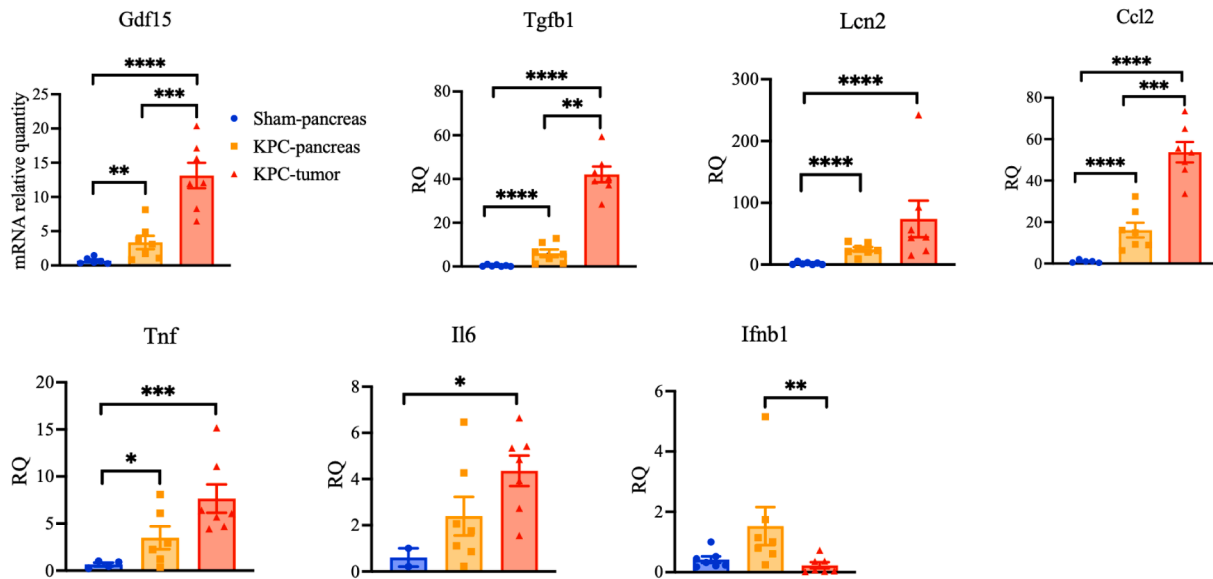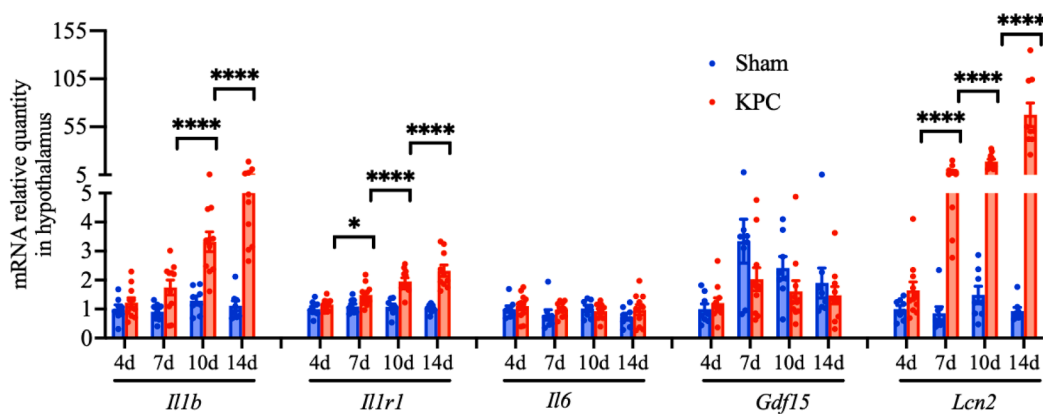

h

Fig. 6. (*continued*).

To comprehensively assess diagnostic and prognostic values of circulating GDF15 and LCN2 in human pancreatic cancer, we conducted animal studies using a well-established mouse model of orthotopic pancreatic KPC tumors. This model accurately replicates clinical manifestations of PDAC [45], and has been extensively studied, demonstrating its organ-specificity, reliability, consistency and reproducibility in mimicking the disease [30,38,39,63,64]. These attributes are crucial to validate findings from animals with relevant clinical implications, ensuring that the translational studies will ultimately benefit cancer patients [40]. Although the mouse model represents a relatively short-term experimental system, considering both mouse and human lifespan and fast progression of PDAC characteristics in clinical setting, it adequately recapitulates key features of the disease process and induces a wide array of cancer manifestations. The mouse studies allowed us to systemically and precisely explore the dynamic change in circulating GDF15 and LCN2 as the tumor grew, cancer progressed, and cachexia developed over a controlled time course. Our data demonstrated that circulating GDF15 and LCN2 elevation in PDAC mice is highly relevant to the clinical disease setting. Furthermore, we conducted a comprehensive examination for pathological alterations at various aspects, including behavioral, organ, tissue, and molecular, thereby illustrating the relationship between potential biomarkers and underlying mechanisms as well as hierarchical causes. In mouse

time-course study, we observed that tumor-bearing mice did not exhibit symptoms during the first week after KPC cell implantation when the tumor was still small (below 0.5 g). However, during the second week, as the tumor underwent exponential growth, tumor-bearing mice displayed sickness behavior and morbidities, including progressive loss of appetite and body mass, lethargy, fatigue, ascites, fat and muscle wasting, and overall decline in body condition. Interestingly, among all the symptoms observed during cancer progression, fatigue (indicated by reduced movement) appeared on day 6 after KPC implantation, which is earlier than any other sickness behaviors, mirroring one of the early chief complaints in many PDAC patients [65]. The extent of fatigue in cancer patients corresponds to a decline in physical function [66].

Cachexia is a devastating wasting syndrome characterized by anorexia, progressive weight loss due to excessive catabolism of muscle and fat tissues, and fatigue. It commonly occurs in advanced diseases, further worsening the underlying condition and reducing treatment tolerance [7,67]. Pancreatic cancer, in particular, has the highest (up to 80 %) incidence of cachexia, and a significant proportion of PDAC patients are diagnosed at an advanced stage with cachexia due to the intrinsic nature of the disease [68]. Pancreatic cancer is characterized by hypovascularization and the presence of a tight desmoplastic stroma around tumor cells, creating a highly hypoxic and nutrient-limited microenvironment [69–71]. This challenging environment forces
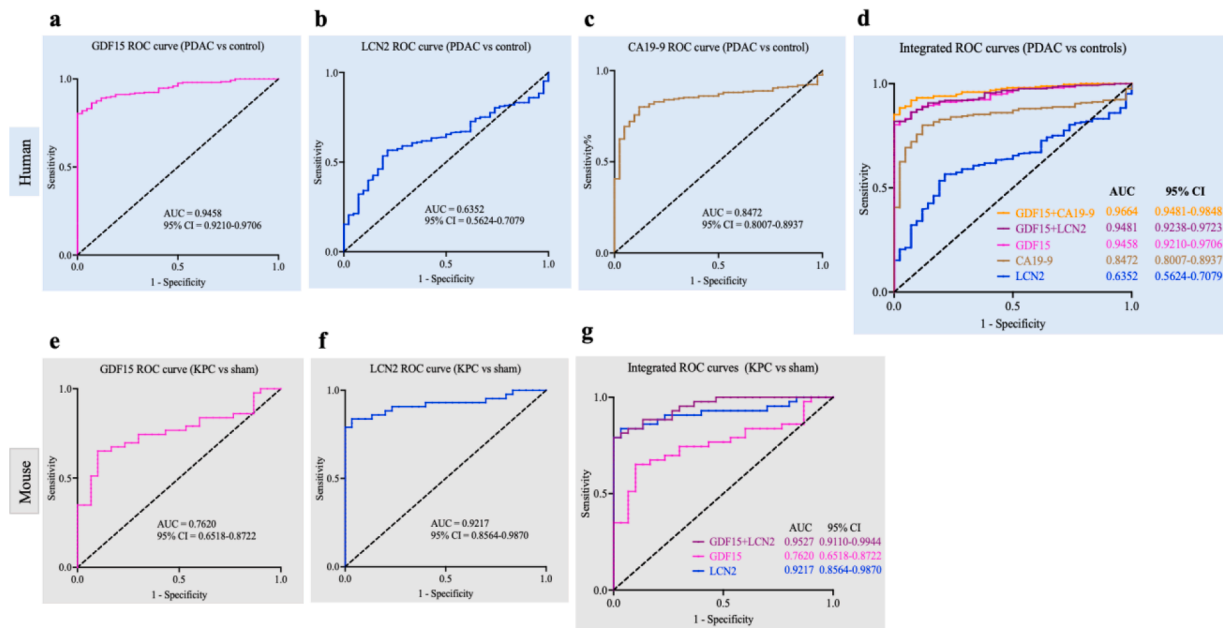
Fig. 7. Assessment of sensitivity and specificity of circulating GDF15 and LCN2 for patients and mice with PDAC. (a-c) ROC curves of GDF15, LCN2, and CA19-9 in PDAC patients vs healthy controls. (d) Integrated ROC curves of GDF15-CA19-9, GDF15-LCN2, and ROC curves of GDF15 alone, LCN2 alone and CA19-9 alone in PADC patients vs healthy controls. (e) and (f) ROC curves of GDF15 and LCN2 in KPC vs sham mice. (g) Integrated ROC curve of GDF15-LCN2, and ROC curves of GDF15 alone and LCN2 alone in KPC vs sham mice. (a-d) PDAC patients, $n = 249$, healthy controls, $n = 42$. (e-g) Sham mice, $n = 30$, KPC mice, $n = 43$.

pancreatic cancer cells to undergo metabolic reprogramming to support uncontrollable proliferation and a tendency for distant metastasis, resulting in increased energy and biosynthetic precursor demands. [4, 71] Consequently, dysregulation in the metabolism of glucose, amino acids, and lipids becomes a hallmark of cachexia [71,72]. Surprisingly, in our human studies, increased GDF15 and LCN2 levels were not correlated with either PDAC patients' SMI or visceral adiposity. One potential explanation for this disconnect is the varying disease stages at the time of blood sampling and CT scans. Another explanation is the controversy regarding the prognostic value of CT-derived muscle and adipose measurements. While some studies propose that local CT scan-derived muscle measurements can predict outcomes in advanced cancer patients [43,44], a most recent study along with other reports have argued against its independent prognostic value for cancer patients, emphasizing instead the role of systemic inflammation [73]. Consequently, our observations also suggest an independent prognostic significance of inflammatory mediators GDF15 and LCN2, but raise doubts about the utility of muscle measurements derived from CT scans. To complement the human studies, we evaluated the dynamic metabolic alterations during PDAC via the mouse time-course study. Starting from the middle stage of PDAC, the tumor-bearing mice displayed predictable phenotypes of muscle and adipose tissue wasting, as well as the upregulation of muscle catabolic gene expression, indicative of progressive cachexia. Correspondingly, the circulating GDF15 and LCN2 levels were remarkably elevated at the cachectic stage, indicating that these molecules are drivers rather than simply biomarkers of cachexia. GDF15, as a cytokine, has context-dependent roles in cancers, depending on the tumor type and micro-environment. It may exert an anti-tumorigenic response to limit tumor growth at the early stages of cancer development, while in the late stages, tumors may utilize GDF15 to evade immune surveillance and expand [24]. On the other hand, LCN2, as a key mediator of anorexia/cachexia, mediates appetite suppression via an MC4R-dependent signaling cascade in CNS during PDAC-associated cachexia [38]. These findings align with separate observations regarding circulating GDF15 or LCN2 levels in patients and rodents with PDAC-associated cachexia [19,20,40]. Despite tremendous progress in the field of cancer cachexia [74], this devastating condition still remains frequently overlooked, underdiagnosed, and under-treated [67].

Therefore, it is imperative to identify biomarkers capable of accurately and readily detecting and predicting cancer and its associated cachexia, ultimately leading to tangible clinical benefits.

A high circulating NLR is recognized as a robust biomarker of poor prognosis in various cancers [52,54]. In this study, we examined the circulating NLR and its association with GDF15 and LCN2 during PDAC. We observed an increased NLR in both PDAC patients and mice. The progressive elevation of NLR in PDAC mice was strongly correlated with the gradual elevation of GDF15 and LCN2 levels. Moreover, in PDAC mice, we observed a dynamic increase in intratumor neutrophils, and highly upregulated inflammatory transcripts in the pancreas, pancreatic tumor, and hypothalamus. These results suggest a rational connection between elevated levels of GDF15, LCN2, and neutrophils, and indicate the severity of inflammation during PDAC encompassing local, central, and systemic aspects. Considering LCN2 is predominantly produced by neutrophils that have emerged as critical regulators of cancer [75], and GDF15's constitutive expression and its ability to be rapidly released upon proteolytic cleavage under stress conditions [17], it is logical to propose that both GDF15 and LCN2 are fast-acting mediators and potent metabolic regulators, involved in neutrophil recruitment, infiltration, migration, and polarization (reprogramming), thereby accelerating inflammation in response to cancer initiation, progression, metastasis, and cachexia development. Surprisingly, in our human studies, although we observed significant increases in NLR, GDF15, LCN2, IL-6, and CA19-9 levels in PDAC patients, NLR was correlated only with LCN2 but not with GDF15, IL-6, or CA19-9. Compared to the mouse studies, this discrepancy is likely due to the unstable nature of neutrophils and the complexity of overall clinical condition in individuals with PDAC, which can dramatically impact NLR. Factors such as non-well-defined disease stages, timing of blood sampling, various treatment statuses including tumor resection, and complications such as infection may contribute to the lack of strong correlations observed in our human studies.

Sensitivity and specificity are classic diagnostic indices of biomarkers [57]. Our sensitivity and specificity analyses demonstrated that circulating GDF15 has higher sensitivity and specificity in diagnosing human PDAC, while circulating LCN2 is more accurate in detecting mouse PDAC. Several factors may explain this distinction. First, animal models cannot fully replicate the complexity of pathophysiological

processes in human diseases particularly in complex cancers. Second, well-controlled conditions in animal experiments may differ from the limited retrospective human studies, and patients often exhibit more heterogeneity than animal models. Last, spontaneous tumors in PDAC patients differ from orthotopically implanted mouse tumors, leading to distinguishable immune responses and tumor-host interactions between patients and mice. These also highlight the insufficiency of relying solely on animal studies for translational investigations and the significant challenges in applying findings from animal studies to clinical trials and, ultimately, clinical practice [76,77]. In this study, we found that the sensitivity and specificity of GDF15, but not LCN2, in both detecting and predicting the prognosis of human PDAC, are more significant than CA19-9. Furthermore, our correlation analyses suggest that GDF15 is a superior predictor for cachexia and survival in PDAC patients. Importantly, our integrated AUC analysis, particularly when assessing the combination of GDF15 and CA19-9, highlights a substantial improvement in sensitivity and specificity. This is consistent with previous studies that explored the use of CA19-9 in combination with other biomarkers [78–81].

In the pursuit of identifying superior biomarkers for pancreatic cancer that offer high sensitivity, specificity, reproducibility, minimal invasiveness, easy of follow-up, cost-effectiveness, and improved patient compliance, recent attention has shifted towards liquid biopsy and diagnostic panels [8,9,12]. Serological biomarkers stand out among all biomarker types due to their simplicity and low risk, making serum the most commonly collected and preferred modality for analysis. However, challenges arise from the complex etiology and pathophysiology of PDAC, as well as patient heterogeneity. In this study, we provide meaningful insights into the role of circulating GDF15 and LCN2 in both PDAC patients and mouse model, focusing on early detection, disease monitoring, and prognosis. These findings have significant implications for diagnostic and prognostic applications. Given the complexity of cancer and the absence of biomarkers with 100 % sensitivity and specificity, we anticipate that combining GDF15 and LCN2 with other biomarkers will improve the accuracy of PDAC diagnosis and prognosis for clinicians. Furthermore, considering the inherent advantages of serological biomarkers, we believe these findings can be practically applied by implementing serum GDF15 and LCN2 tests for PDAC screening and routine examinations. The importance of early detection and accurate prognosis of cancer cannot be emphasized enough, as it can significantly impact patient outcomes. We are confident that our findings will contribute to advancing early detection and prediction strategies for pancreatic cancer.

This study had several key limitations, primarily due to the retrospective nature of human sample collection and the potential biases that come with it. During our investigation, we encountered incomplete historical information and inconsistent test results in the patients' charts, such as variations in sample collection times and intervals, as well as missing descriptions of disease stages and specific testing items of interest. These issues led to the exclusion of certain samples or data, which may have introduced biases. Additionally, there was a lack of human samples from multiple medical sites, limiting the ability to further validate our findings. To address these limitations, a prospective human study with larger cohorts conducted across multiple sites will be necessary.

Conclusion

This study suggests that GDF15 is a promising biomarker for the early detection and prognosis of PDAC, while LCN2 could strengthen diagnostic panels. These findings are anticipated to significantly influence the advancement of strategies for early detection and prognostic evaluation in PDAC, potentially leading to better outcomes for pancreatic cancer patients. To validate and confirm these results, future research should focus on larger-scale prospective human studies conducted across multiple sites.

Data sharing statement

All data associated with this study are available in the main text, main figures, and supplemental materials. There are no restrictions on data availability. Supporting data values and Image files are available upon reasonable request.

CRediT authorship contribution statement

Xinxia Zhu: Writing – review & editing, Writing – original draft, Project administration, Methodology, Investigation, Formal analysis, Data curation, Conceptualization. **Brennan Olson:** Methodology, Investigation, Formal analysis, Data curation. **Dove Keith:** Resources, Data curation. **Mason A Norgard:** Investigation, Data curation. **Peter R Levasseur:** Investigation, Data curation. **Parham Diba:** Investigation. **Sara Protzek:** Data curation. **Ju Li:** Investigation. **Xiaolin Li:** Validation. **Tetiana Korzun:** Validation. **Ariana L Sattler:** Validation. **Abigail C Buenafe:** Validation. **Aaron J Grossberg:** Writing – review & editing, Validation. **Daniel L Marks:** Writing – review & editing, Validation, Supervision, Resources, Funding acquisition, Formal analysis, Data curation, Conceptualization.

Declaration of competing interest

The authors declare the following financial interests/personal relationships which may be considered as potential competing interests:

Daniel L Marks reports financial support was provided by NIH NCI. Daniel L Marks reports a relationship with Endevica Bio, Inc that includes: equity or stocks and funding grants. Daniel L Marks reports a relationship with Alkermes Inc that includes: consulting or advisory. Daniel L Marks reports a relationship with Pfizer Inc that includes: consulting or advisory. If there are other authors, they declare that they have no known competing financial interests or personal relationships that could have appeared to influence the work reported in this paper.

Xinxia Zhu reports a relationship with Endevica Bio, Inc that includes: equity or stocks. If there are other authors, they declare that they have no known competing financial interests or personal relationships that could have appeared to influence the work reported in this paper.

The authors declare that they have no known competing financial interests or personal relationships that could have appeared to influence the work reported in this paper.

Brennan Olson, Dove Keith, Mason A Norgard, Peter R Levasseur, Parham Diba, Sara Protzek, Ju Li, Xiaolin Li, Tetiana Korzun, Ariana L Sattler, Abigail C Buenafe, Aaron J Grossberg

Supplementary materials

Supplementary material associated with this article can be found, in the online version, at doi:10.1016/j.tranon.2024.102129.

References

[1] A.J. Grossberg, L.C. Chu, C.R. Deig, E.K. Fishman, W.L. Hwang, A. Maitra, D. L. Marks, A. Mehta, N. Nabavizadeh, D.M. Simeone, et al., Multidisciplinary standards of care and recent progress in pancreatic ductal adenocarcinoma, CA Cancer J. Clin. 70 (2020) 375–403, https://doi.org/10.3322/caac.21626.

[2] J.D. Mizrahi, R. Surana, J.W. Valle, R.T. Shroff, Pancreatic cancer, Lancet 395 (2020) 2008–2020, https://doi.org/10.1016/s0140-6736(20)30974-0.

[3] Z. Zhou, B.H. Edil, M. Li, Combination therapies for cancer: challenges and opportunities, BMC Med. 21 (2023) 171, https://doi.org/10.1186/s12916-023-02852-4.

[4] C.J. Halbrook, C.A. Lyssiotis, M. Pasca di Magliano, A. Maitra, Pancreatic cancer: advances and challenges, Cell 186 (2023) 1729–1754, https://doi.org/10.1016/j.cell.2023.02.014.

[5] R.L. Siegel, K.D. Miller, N.S. Wagle, A. Jemal, Cancer statistics, 2023, CA Cancer J. Clin. 73 (2023) 17–48, https://doi.org/10.3322/caac.21763.

[6] D.R. Principe, P.W. Underwood, M. Korc, J.G. Trevino, H.G. Munshi, A Rana, The current treatment paradigm for pancreatic ductal adenocarcinoma and barriers to therapeutic efficacy, Front. Oncol. 11 (2021) 688377, https://doi.org/10.3389/fonc.2021.688377.

[7] V.E. Baracos, L. Martin, M. Korc, D.C. Guttridge, K.C.H. Fearon, Cancer-associated cachexia, Nat. Rev. Dis. Primers 4 (2018) 17105, https://doi.org/10.1038/nrdp.2017.105.

[8] M.J. Amaral, R.C. Oliveira, P. Donato, J.G. Tralhão, Pancreatic cancer biomarkers: oncogenic mutations, tissue and liquid biopsies, and radiomics-a review, Dig. Dis. Sci. 68 (2023) 2811–2823, https://doi.org/10.1007/s10620-023-07904-6.

[9] R.S. O'Neill, A. Stoita, Biomarkers in the diagnosis of pancreatic cancer: are we closer to finding the golden ticket? World J. Gastroenterol. 27 (2021) 4045–4087, https://doi.org/10.3748/wjg.v27.i26.4045.

[10] R.E. Brand, B.M. Nolen, H.J. Zeh, P.J. Allen, M.A. Eloubeidi, M. Goldberg, E. Elton, J.P. Arnoletti, J.D. Christein, S.M. Vickers, et al., Serum biomarker panels for the detection of pancreatic cancer, Clin. Cancer Res. 17 (2011) 805–816, https://doi.org/10.1158/1078-0432.Ccr-10-0248.

[11] J. Yang, R. Xu, C. Wang, J. Qiu, B. Ren, L. You, Early screening and diagnosis strategies of pancreatic cancer: a comprehensive review, Cancer Commun. (Lond) 41 (2021) 1257–1274, https://doi.org/10.1002/cac2.12204.

[12] H. Wu, S. Ou, H. Zhang, R. Huang, S. Yu, M. Zhao, S. Tai, Advances in biomarkers and techniques for pancreatic cancer diagnosis, Cancer Cell Int. 22 (2022) 220, https://doi.org/10.1186/s12935-022-02640-9.

[13] L.E. Kane, G.S. Mellotte, E. Mylod, R.M. O'Brien, F. O'Connell, C.E. Buckley, J. Arlow, K. Nguyen, D. Mockler, A.D. Meade, et al., Diagnostic accuracy of blood-based biomarkers for pancreatic cancer: a systematic review and meta-analysis, Cancer Res. Commun. 2 (2022) 1229–1243, https://doi.org/10.1158/2767-9764.Crc-22-0190.

[14] M.R. Bootcov, A.R. Bauskin, S.M. Valenzuela, A.G. Moore, M. Bansal, X.Y. He, H. P. Zhang, M. Donnellan, S. Mahler, K. Pryor, et al., MIC-1, a novel macrophage inhibitory cytokine, is a divergent member of the TGF-beta superfamily, Proc. Natl. Acad. Sci. USA 94 (1997) 11514–11519, https://doi.org/10.1073/pnas.94.21.11514.

[15] T. Ling, J. Zhang, F. Ding, L. Ma, Role of growth differentiation factor 15 in cancer cachexia (Review), Oncol. Lett. 26 (2023) 462, https://doi.org/10.3892/ol.2023.14049.

[16] J.A. Siddiqui, R. Pothuraju, P. Khan, G. Sharma, S. Muniyan, P. Seshacharyulu, M. Jain, M.W. Nasser, S.K. Batra, Pathophysiological role of growth differentiation factor 15 (GDF15) in obesity, cancer, and cachexia, Cytokine Growth Factor Rev. 64 (2022) 71–83, https://doi.org/10.1016/j.cytogfr.2021.11.002.

[17] J. Wischhusen, I. Melero, W.H. Fridman, Growth/Differentiation factor-15 (GDF-15): from biomarker to novel targetable immune checkpoint, Front. Immunol. 11 (2020) 951, https://doi.org/10.3389/fimmu.2020.00951.

[18] M. Guo, H. Zhao, Growth differentiation factor-15 may be a novel biomarker in pancreatic cancer: a review, Medicine 103 (2024) e36594, https://doi.org/10.1097/md.0000000000036594.

[19] X. Wang, Y. Li, H. Tian, J. Qi, M. Li, C. Fu, F. Wu, Y. Wang, D. Cheng, W. Zhao, et al., Macrophage inhibitory cytokine 1 (MIC-1/GDF15) as a novel diagnostic serum biomarker in pancreatic ductal adenocarcinoma, BMC Cancer 14 (2014) 578, https://doi.org/10.1186/1471-2407-14-578.

[20] Z. Zhao, J. Zhang, L. Yin, J. Yang, Y. Zheng, M. Zhang, B. Ni, H Wang, Upregulated GDF-15 expression facilitates pancreatic ductal adenocarcinoma progression through orphan receptor GFRAL, Aging 12 (2020) 22564–22581, https://doi.org/10.18632/aging.103830.

[21] T. Borner, E.D. Shaulson, M.Y. Ghidewon, A.B. Barnett, C.C. Horn, R.P. Doyle, H. J. Grill, M.R. Hayes, B.C. De Jonghe, GDF15 induces anorexia through nausea and emesis, Cell Metab. 31 (2020) 351–362, https://doi.org/10.1016/j.cmet.2019.12.004, e355.

[22] J.Y. Hsu, S. Crawley, M. Chen, D.A. Ayupova, D.A. Lindhout, J. Higbee, A. Kutach, W. Joo, Z. Gao, D. Fu, et al., Erratum: non-homeostatic body weight regulation through a brainstem-restricted receptor for GDF15, Nature 551 (2017) 398, https://doi.org/10.1038/nature24481.

[23] L. Yang, C.C. Chang, Z. Sun, D. Madsen, H. Zhu, S.B. Padkjær, X. Wu, T. Huang, K. Hultman, S.J. Paulsen, et al., GFRAL is the receptor for GDF15 and is required for the anti-obesity effects of the ligand, Nat. Med. 23 (2017) 1158–1166, https://doi.org/10.1038/nm.4394.

[24] D.S. Ahmed, S. Isnard, J. Lin, B. Routy, J.P. Routy, GDF15/GFRAL pathway as a metabolic signature for cachexia in patients with cancer, J. Cancer 12 (2021) 1125–1132, https://doi.org/10.7150/jca.50376.

[25] H. Johnen, S. Lin, T. Kuffner, D.A. Brown, V.W. Tsai, A.R. Bauskin, L. Wu, G. Pankhurst, L. Jiang, S. Junankar, et al., Tumor-induced anorexia and weight loss are mediated by the TGF-beta superfamily cytokine MIC-1, Nat. Med. 13 (2007) 1333–1340, https://doi.org/10.1038/nm1677.

[26] C. Li, J. Wang, J. Kong, J. Tang, Y. Wu, E. Xu, H. Zhang, M. Lai, GDF15 promotes EMT and metastasis in colorectal cancer, Oncotarget 7 (2016) 860–872, https://doi.org/10.18632/oncotarget.6205.

[27] A.C. Staff, J. Trovik, A.G. Eriksson, E. Wik, K.C. Wollert, T. Kempf, H.B. Salvesen, Elevated plasma growth differentiation factor-15 correlates with lymph node metastases and poor survival in endometrial cancer, Clin. Cancer Res. 17 (2011) 4825–4833, https://doi.org/10.1158/1078-0432.Ccr-11-0715.

[28] V.W.W. Tsai, Y. Husaini, A. Sainsbury, D.A. Brown, S.N. Breit, The MIC-1/GDF15-GFRAL pathway in energy homeostasis: implications for obesity, cachexia, and other associated diseases, Cell Metab. 28 (2018) 353–368, https://doi.org/10.1016/j.cmet.2018.07.018.

[29] D. Wang, L.K. Townsend, G.J. DesOrmeaux, S.M. Frangos, B. Batchuluun, L. Dumont, R.E. Kuhre, E. Ahmadi, S. Hu, I.A. Rebalka, et al., GDF15 promotes weight loss by enhancing energy expenditure in muscle, Nature 619 (2023) 143–150, https://doi.org/10.1038/s41586-023-06249-4.

[30] X. Zhu, K.G. Burfeind, K.A. Michaelis, T.P. Braun, B. Olson, K.R. Pelz, T.K. Morgan, D.L. Marks, MyD88 signalling is critical in the development of pancreatic cancer cachexia, J. Cachexia Sarcopenia Muscle 10 (2019) 378–390, https://doi.org/10.1002/jcsm.12377.

[31] T.H. Flo, K.D. Smith, S. Sato, D.J. Rodriguez, M.A. Holmes, R.K. Strong, S. Akira, A Aderem, Lipocalin 2 mediates an innate immune response to bacterial infection by sequestrating iron, Nature 432 (2004) 917–921, https://doi.org/10.1038/nature03104.

[32] A.R. Moschen, T.E. Adolph, R.R. Gerner, V. Wieser, H. Tilg, Lipocalin-2: a master mediator of intestinal and metabolic inflammation, Trends. Endocrinol. Metab. 28 (2017) 388–397, https://doi.org/10.1016/j.tem.2017.01.003.

[33] S.B. Gomez-Chou, A.K. Swidnicka-Siergiejko, N. Badi, M. Chavez-Tomar, G. B. Lesinski, T. Bekaii-Saab, M.R. Farren, T.A. Mace, C. Schmidt, Y. Liu, et al., Lipocalin-2 promotes pancreatic ductal adenocarcinoma by regulating inflammation in the tumor microenvironment, Cancer Res. 77 (2017) 2647–2660, https://doi.org/10.1158/0008-5472.Can-16-1986.

[34] A. Viau, K. El Karoui, D. Laouari, M. Burtin, C. Nguyen, K. Mori, E. Pillebout, T. Berger, T.W. Mak, B. Knebelmann, et al., Lipocalin 2 is essential for chronic kidney disease progression in mice and humans, J. Clin. Invest. 120 (2010) 4065–4076, https://doi.org/10.1172/jci42004.

[35] A. Yndestad, L. Landrø, T. Ueland, C.P. Dahl, T.H. Flo, L.E. Vinge, T. Espevik, S. S. Frøland, C. Husberg, G. Christensen, et al., Increased systemic and myocardial expression of neutrophil gelatinase-associated lipocalin in clinical and experimental heart failure, Eur. Heart. J. 30 (2009) 1229–1236, https://doi.org/10.1093/eurheartj/ehp088.

[36] V. Abella, M. Scotece, J. Conde, R. Gómez, A. Lois, J. Pino, J.J. Gómez-Reino, F. Lago, A. Mobasheri, O. Gualillo, The potential of lipocalin-2/NGAL as biomarker for inflammatory and metabolic diseases, Biomarkers 20 (2015) 565–571, https://doi.org/10.3109/1354750x.2015.1123354.

[37] G.S. Santiago-Sánchez, V. Pita-Grisanti, B. Quiñones-Díaz, K. Gumpper, Z. Cruz-Monserrate, P.E. Vivas-Mejía, Biological functions and therapeutic potential of lipocalin 2 in cancer, Int. J. Mol. Sci. 21 (2020), https://doi.org/10.3390/ijms21124365.

[38] B. Olson, X. Zhu, M.A. Norgard, P.R. Levasseur, J.T. Butler, A. Buenafe, K. G. Burfeind, K.A. Michaelis, K.R. Pelz, H. Mendez, et al., Lipocalin 2 mediates appetite suppression during pancreatic cancer cachexia, Nat. Commun. 12 (2021) 2057, https://doi.org/10.1038/s41467-021-22361-3.

[39] B. Olson, X. Zhu, M.A. Norgard, P. Diba, P.R. Levasseur, A.C. Buenafe, C. Huisman, K.G. Burfeind, K.A. Michaelis, G. Kong, et al., Chronic cerebral lipocalin 2 exposure elicits hippocampal neuronal dysfunction and cognitive impairment, Brain Behav. Immun. 97 (2021) 102–118, https://doi.org/10.1016/j.bbi.2021.07.002.

[40] E.E. Talbert, D.C. Guttridge, Emerging signaling mediators in the anorexia-cachexia syndrome of cancer, Trends Cancer 8 (2022) 397–403, https://doi.org/10.1016/j.trecan.2022.01.004.

[41] O. Adler, Y. Zait, N. Cohen, R. Blazquez, H. Doron, L. Monteran, Y. Scharff, T. Shami, D. Mundhe, G. Glehr, et al., Reciprocal interactions between innate immune cells and astrocytes facilitate neuroinflammation and brain metastasis via lipocalin-2, Nat. Cancer 4 (2023) 401–418, https://doi.org/10.1038/s43018-023-00519-w.

[42] K. Popuri, D. Cobzas, N. Esfandiari, V. Baracos, M Jägersand, Body composition assessment in axial CT images using FEM-based automatic segmentation of skeletal muscle, IEEe Trans. Med. ImAging 35 (2016) 512–520, https://doi.org/10.1109/tmi.2015.2479252.

[43] M. Mourtzakis, C.M. Prado, J.R. Lieffers, T. Reiman, L.J. McCargar, V.E. Baracos, A practical and precise approach to quantification of body composition in cancer patients using computed tomography images acquired during routine care, Appl. Physiol. Nutr. Metab. 33 (2008) 997–1006, https://doi.org/10.1139/h08-075.

[44] C.M. Prado, L.A. Birdsell, V.E. Baracos, The emerging role of computerized tomography in assessing cancer cachexia, Curr. Opin. Support. Palliat. Care 3 (2009) 269–275, https://doi.org/10.1097/SPC.0b013e328331124a.

[45] K.A. Michaelis, X. Zhu, K.G. Burfeind, S.M. Krasnow, P.R. Levasseur, T.K. Morgan, D.L. Marks, Establishment and characterization of a novel murine model of pancreatic cancer cachexia, J. Cachexia Sarcopenia Muscle 8 (2017) 824–838, https://doi.org/10.1002/jcsm.12225.

[46] M. Ogłuszka, M. Orzechowska, D. Jędroszka, P. Witas, A.K. Bednarek, Evaluate Cutpoints: adaptable continuous data distribution system for determining survival

in Kaplan-Meier estimator, Comput. Methods Programs Biomed. 177 (2019) 133–139, https://doi.org/10.1016/j.cmpb.2019.05.023.

[47] R. Holmer, F.A. Goumas, G.H. Waetzig, S. Rose-John, H. Kalthoff, Interleukin-6: a villain in the drama of pancreatic cancer development and progression, Hepatobiliary. Pancreat. Dis. Int. 13 (2014) 371–380, https://doi.org/10.1016/s1499-3872(14)60259-9.

[48] F. Shen, C. Liu, W. Zhang, S. He, F. Wang, J. Wang, Q. Li, F. Zhou, Serum levels of IL-6 and CRP can predict the efficacy of mFOLFIRINOX in patients with advanced pancreatic cancer, Front. Oncol. 12 (2022) 964115, https://doi.org/10.3389/fonc.2022.964115.

[49] N. Vainer, C. Dehlendorff, J.S. Johansen, Systematic literature review of IL-6 as a biomarker or treatment target in patients with gastric, bile duct, pancreatic and colorectal cancer, Oncotarget 9 (2018) 29820–29841, https://doi.org/10.18632/oncotarget.25661.

[50] Z.V. Fong, J.M. Winter, Biomarkers in pancreatic cancer: diagnostic, prognostic, and predictive, Cancer J. 18 (2012) 530–538, https://doi.org/10.1097/PPO.0b013e31827654ea.

[51] A.D. Kjaergaard, I.M. Chen, A.Z. Johansen, B.G. Nordestgaard, S.E. Bojesen, J. S. Johansen, Inflammatory biomarker score identifies patients with six-fold increased risk of one-year mortality after pancreatic cancer, Cancers 13 (2021), https://doi.org/10.3390/cancers13184599.

[52] M.E. Shaul, Z.G. Fridlender, Tumour-associated neutrophils in patients with cancer, Nat. Rev. Clin. Oncol. 16 (2019) 601–620, https://doi.org/10.1038/s41571-019-0222-4.

[53] A.J. McFarlane, F. Fercoq, S.B. Coffelt, L.M. Carlin, Neutrophil dynamics in the tumor microenvironment, J. Clin. Invest. 131 (2021), https://doi.org/10.1172/jci143759.

[54] S. Xiong, L. Dong, L. Cheng, Neutrophils in cancer carcinogenesis and metastasis, J. Hematol. Oncol. 14 (2021) 173, https://doi.org/10.1186/s13045-021-01187-y.

[55] G. Luo, M. Guo, Z. Liu, Z. Xiao, K. Jin, J. Long, L. Liu, C. Liu, J. Xu, Q. Ni, X Yu, Blood neutrophil-lymphocyte ratio predicts survival in patients with advanced pancreatic cancer treated with chemotherapy, Ann. Surg. Oncol. 22 (2015) 670–676, https://doi.org/10.1245/s10434-014-4021-y.

[56] Q. Zhang, M.M. Song, X. Zhang, J.S. Ding, G.T. Ruan, X.W. Zhang, T. Liu, M. Yang, Y.Z. Ge, M. Tang, et al., Association of systemic inflammation with survival in patients with cancer cachexia: results from a multicentre cohort study, J. Cachexia Sarcopenia Muscle 12 (2021) 1466–1476, https://doi.org/10.1002/jcsm.12761.

[57] P. Ray, Y. Le Manach, B. Riou, T.T. Houle, Statistical evaluation of a biomarker, Anesthesiology 112 (2010) 1023–1040, https://doi.org/10.1097/ALN.0b013e3181d47604.

[58] S. Okada, T. Okusaka, H. Ishii, A. Kyogoku, M. Yoshimori, N. Kajimura, K. Yamaguchi, T. Kakizoe, Elevated serum interleukin-6 levels in patients with pancreatic cancer, Jpn. J. Clin. Oncol. 28 (1998) 12–15, https://doi.org/10.1093/jjco/28.1.12.

[59] M. Ikeda, S. Okada, K. Tokuuye, H. Ueno, T. Okusaka, Prognostic factors in patients with locally advanced pancreatic carcinoma receiving chemoradiotherapy, Cancer 91 (2001) 490–495, https://doi.org/10.1002/1097-0142(20010201)91:3<490::aid-cncr1027>3.0.co;2-l.

[60] H.W. Kim, J.C. Lee, K.H. Paik, J. Kang, J. Kim, J.H. Hwang, Serum interleukin-6 is associated with pancreatic ductal adenocarcinoma progression pattern, Medicine 96 (2017) e5926, https://doi.org/10.1097/md.0000000000005926.

[61] N. Unver, F. McAllister, IL-6 family cytokines: key inflammatory mediators as biomarkers and potential therapeutic targets, Cytokine Growth Factor Rev. 41 (2018) 10–17, https://doi.org/10.1016/j.cytogfr.2018.04.004.

[62] G. van Duijneveldt, M.D.W. Griffin, T.L. Putoczki, Emerging roles for the IL-6 family of cytokines in pancreatic cancer, Clin. Sci. 134 (2020) 2091–2115, https://doi.org/10.1042/cs20191211.

[63] K.G. Burfeind, X. Zhu, M.A. Norgard, P.R. Levasseur, C. Huisman, A.C. Buenafe, B. Olson, K.A. Michaelis, E.R. Torres, S. Jeng, et al., Circulating myeloid cells invade the central nervous system to mediate cachexia during pancreatic cancer, Elife 9 (2020), https://doi.org/10.7554/eLife.54095.

[64] K.G. Burfeind, X. Zhu, M.A. Norgard, P.R. Levasseur, C. Huisman, K.A. Michaelis, B. Olson, D.L. Marks, Microglia in the hypothalamus respond to tumor-derived

factors and are protective against cachexia during pancreatic cancer, Glia 68 (2020) 1479–1494, https://doi.org/10.1002/glia.23796.

[65] M. Di Marco, I. Rubbi, A. Baldi, R. Di Lorenzo, D. Magnani, V. Cremonini, L. Sarli, G. Artioli, P. Ferri, Evaluation of fatigue in patients with pancreatic cancer receiving chemotherapy treatment: a cross-sectional observational study, Acta Biomed. 89 (2018) 18–27, https://doi.org/10.23750/abm.v89i4-S.7063.

[66] J. McDonald, J. Sayers, S.D. Anker, J. Arends, T.R. Balstad, V. Baracos, L. Brown, A. Bye, O. Dajani, R. Dolan, et al., Physical function endpoints in cancer cachexia clinical trials: systematic Review 1 of the cachexia endpoints series, J. Cachexia Sarcopenia Muscle (2023), https://doi.org/10.1002/jcsm.13321.

[67] M. Ferrer, T.G. Anthony, J.S. Ayres, G. Biffi, J.C. Brown, B.J. Caan, E.M. Cespedes Feliciano, A.P. Coll, R.F. Dunne, M.D. Goncalves, et al., Cachexia: a systemic consequence of progressive, unresolved disease, Cell 186 (2023) 1824–1845, https://doi.org/10.1016/j.cell.2023.03.028.

[68] I. Ozola Zalite, R. Zykus, M. Francisco Gonzalez, F. Saygili, A. Pukitis, S. Gaujoux, R.M. Charnley, V. Lyadov, Influence of cachexia and sarcopenia on survival in pancreatic ductal adenocarcinoma: a systematic review, Pancreatology. 15 (2015) 19–24, https://doi.org/10.1016/j.pan.2014.11.006.

[69] C.M. Sousa, A.C. Kimmelman, The complex landscape of pancreatic cancer metabolism, Carcinogenesis 35 (2014) 1441–1450, https://doi.org/10.1093/carcin/bgu097.

[70] J. Yang, B. Ren, G. Yang, H. Wang, G. Chen, L. You, T. Zhang, Y. Zhao, The enhancement of glycolysis regulates pancreatic cancer metastasis, Cell Mol. Life Sci. 77 (2020) 305–321, https://doi.org/10.1007/s00018-019-03278-z.

[71] S. Wang, Y. Zheng, F. Yang, L. Zhu, X.Q. Zhu, Z.F. Wang, X.L. Wu, C.H. Zhou, J. Y. Yan, B.Y. Hu, et al., The molecular biology of pancreatic adenocarcinoma: translational challenges and clinical perspectives, Signal. Transduct. Target. Ther. 6 (2021) 249, https://doi.org/10.1038/s41392-021-00659-4.

[72] D. Hanahan, R.A. Weinberg, Hallmarks of cancer: the next generation, Cell 144 (2011) 646–674, https://doi.org/10.1016/j.cell.2011.02.013.

[73] J. McGovern, R.D. Dolan, C. Simmons, L.E. Daly, A.M. Ryan, D.G. Power, M. T. Fallon, B.J. Laird, D.C. McMillan, Are CT-derived muscle measurements prognostic, independent of systemic inflammation, in good performance status patients with advanced cancer? Cancers 15 (2023) https://doi.org/10.3390/cancers15133407.

[74] B.J.A. Laird, A. Jatoi, Cancer cachexia: learn from yesterday, live for today and hope for tomorrow, Curr. Opin. Support. Palliat. Care 17 (2023) 161, https://doi.org/10.1097/spc.0000000000000652.

[75] C.C. Hedrick, I. Malanchi, Neutrophils in cancer: heterogeneous and multifaceted, Nat. Rev. Immunol. 22 (2022) 173–187, https://doi.org/10.1038/s41577-021-00571-6.

[76] A. Choudhary, J.A. Ibdah, Animal models in today's translational medicine world, Mo Med. 110 (2013) 220–222.

[77] C.H.C. Leenaars, C. Kouwenaar, F.R. Stafleu, A. Bleich, M. Ritskes-Hoitinga, R.B. M. De Vries, F.L.B. Meijboom, Animal to human translation: a systematic scoping review of reported concordance rates, J. Transl. Med. 17 (2019) 223, https://doi.org/10.1186/s12967-019-1976-2.

[78] S.H. Jiang, D. Liu, L.P. Hu, S. Zhang, Y. Yu, Y.W. Sun, J. Ji, Z.G. Zhang, Modeling of cancer-related body-wide effects identifies LTB4 as a diagnostic biomarker for pancreatic cancer, EBioMedicine 80 (2022) 104050, https://doi.org/10.1016/j.ebiom.2022.104050.

[79] S. Kaur, L.M. Smith, A. Patel, M. Menning, D.C. Watley, S.S. Malik, S.R. Krishn, K. Mallya, A. Aithal, A.R. Sasson, et al., A combination of MUC5AC and CA19-9 improves the diagnosis of pancreatic cancer: a multicenter study, Am. J. Gastroenterol. 112 (2017) 172–183, https://doi.org/10.1038/ajg.2016.482.

[80] H. Kim, K.N. Kang, Y.S. Shin, Y. Byun, Y. Han, W. Kwon, C.W. Kim, J.Y. Jang, Biomarker panel for the diagnosis of pancreatic ductal adenocarcinoma, Cancers 12 (2020), https://doi.org/10.3390/cancers12061443.

[81] J. Liu, J. Gao, Y. Du, Z. Li, Y. Ren, J. Gu, X. Wang, Y. Gong, W. Wang, X. Kong, Combination of plasma microRNAs with serum CA19-9 for early detection of pancreatic cancer, Int. J. Cancer 131 (2012) 683–691, https://doi.org/10.1002/ijc.26422.